

A Semisupervised Deep Learning Neural Network Using Pseudolabels for Three-Dimensional Shallow Strata Modelling and Uncertainty Analysis in Urban Areas from Borehole Data

~~Semisupervised Deep Learning Neural Network Using Pseudolabels for Three-dimensional Urban Geological Modelling and Uncertainty Analysis from Borehole Data~~

Jiateng Guo^{1*}, Xuechuang Xu¹, [Luyuan Wang¹](mailto:wangluyuan9@163.com), Xulei Wang¹, Lixin Wu², Mark Jessell³, Vitaliy Ogarko³, Zhibin Liu¹ and Yufei Zheng¹

¹College of Resources and Civil Engineering, Northeastern University, Shenyang, China; 2000985@stu.neu.edu.cn (X. X.); wangluyuan9@163.com (L. W.); wxldbdx@163.com (X. W.); 207158587@qq.com (Z. L.); 15333134708@163.com (Y. Z.)

²School of Geosciences and Info-Physics, Central South University, Lushan Nanlu 932, Yuelu District, Changsha 410012, China; awulixin@263.net (L. W.)

³Centre for Exploration Targeting / Mineral Exploration Cooperative Research Centre / DARE Centre, School of Earth Sciences, The University of Western Australia, Perth, Australia; mark.jessell@uwa.edu.au (M. J.); vitaliy.ogarko@uwa.edu.au (V. O.)

*Correspondence to: Jiateng Guo (guojiateng@mail.neu.edu.cn; Tel.: +86-24-8368-7693)

Abstract. Borehole data are essential for conducting precise urban geological surveys and large-scale geological investigations. Traditionally, explicit and implicit modelling have been the primary methods for visualizing borehole data and constructing 3D geological models. However, explicit modelling requires substantial manual labour, while implicit modelling faces challenges related to uncertainty. Recently, machine learning approaches have emerged as effective solutions to address these issues in 3D geological modelling. Nevertheless, the use of machine learning to build 3D geological models is often limited by insufficient training data. In this paper, we propose the semisupervised deep learning using pseudolabels (SDLP) algorithm to overcome the issue of insufficient training data. Specifically, we construct the pseudolabels in the training dataset using the triangular irregular network (TIN) method. A 3D geological model is constructed using borehole data obtained from a geological survey of urban areas in Shenyang, Liaoning Province, NE China. Additionally, we compare the results of the 3D geological model built based on SDLP with those obtained from a support vector machine (SVM) method and an implicit HRBF modelling method. The findings demonstrate that our proposed method effectively resolves issues with insufficient training data. Moreover, compared to the 3D geological models constructed using the HRBF algorithm and SVM algorithm, the 3D geological model built based on the SDLP algorithm better conforms to the sedimentation patterns of the region and supports uncertainty analysis. In conclusion, the semisupervised deep learning method with pseudolabelling proposed in this paper provides a solution for 3D geological modelling in sparsely distributed areas with borehole data.

Abstract. Boreholes are one of the main tools for high precision urban geology exploration and large-scale geological investigations. At present, machine learning based 3D geological modelling methods for borehole data have difficulty building a finer and more complex model and analysing the modelling results with uncertainty. In this paper, a semisupervised learning algorithm using pseudolabels for 3D geological modelling from borehole data is proposed. We establish a 3D geological model using borehole data from a complex real urban local survey area in Shenyang, and the modelling results are compared with implicit surface modelling and traditional machine learning modelling methods. Finally, an uncertainty analysis of the model is made. The results show that the method effectively expands the sample space, the

Formatted: Font: Bold

40 modelling results perform well in terms of spatial morphology and geological semantics, and the proposed modelling method
can achieve good modelling results for more complex geological regions.

1. Introduction

45 Three-dimensional (3D) urban geological models are digital representations of subsurface strata and their associated features
(Houlding, 1994). In recent years, the utilization of 3D geological models has expanded across various geological fields,
such as mineral exploration (Zhang et al., 2021), geological storage (Thanh et al., 2019), groundwater resource estimation
(Thibaut et al., 2021), geological disaster early warning generation (Høyer et al., 2019; Livani et al., 2022), and engineering
geological condition evaluation (Chen et al., 2018; Guo et al., 2021; Lyu et al., 2021; Marz'an et al., 2021).

50 Geological spatial distribution has complexity, fuzziness and uncertainty. To reasonably arrange urban engineering
construction, the underground situation of each area of a city needs to be understood and a comprehensive assessment
carried out. The establishment of a reasonable 3D geological model, intuitive expression of geological features, display of
underground geological structures, and revelation of the spatial distribution law are important foundations to ensure
engineering design and implementation. The stratum structure is the result of a long geological process, and its spatial and
temporal distribution is uneven and irregular. At present, it is still difficult to summarize a set of reasonable mathematical
laws to express the stratum distribution. Deep learning methods can obtain the complex mapping relationship between input
55 and output by relying on the powerful computing power of computers, which has been applied in many complex fields and
has increasingly attracted the attention of geological researchers, such as 3D modelling.

60 The commonly used data for 3D geological modelling include borehole data, geophysical data, survey and mapping
data, and other types of data. Among these, borehole data provide the most accurate reflection of subsurface geological
information (Guo et al., 2022). Notably, 3D geological modelling from borehole data can be divided into explicit modelling
and implicit modelling (Jessell, 2001; Caumon et al., 2007; Wang et al., 2018). The explicit modelling approach can be used
to directly delineate geological formations and interpret tectonics based on borehole data. Explicit 3D geological modelling
methods are widely used in the 3D modelling of mines and regional geological structures, and they include the interactive
3D forward modelling method (Yang et al., 2011), generalized tri-prism (GTP) modelling method (Wu et al., 2004; Che et
al., 2009) and parametric surface method (Lyu et al., 2021). However, these approaches heavily relies on the expertise of
65 geologists and often proves time-consuming and labour-intensive when dealing with large-scale borehole data.

70 Implicit modelling methods are used to construct a 3D geological model by establishing the implicit equation of the
isosurface representing the geometric shape of a geological body and using a series of implicit function visualization
methods (Jessell M. et al., 2022). That is, a complex 3D geological object is represented as a continuous function of
geological coordinates (Wang G.W. et al., 2011; Zhong D. Y. et al., 2021). This method does not require extensive human-
computer interaction and has the advantages of high modelling accuracy, excellent smoothness and high spatial analysis
efficiency (Sun H. et al., 2023). It is widely used in the field of geological modelling (Hillier M. J. et al., 2014; Calcagno P.
et al., 2008; Shi T. D. et al., 2021) and provides results to complement the results of most urban geological surveys (de la
Varga M. et al., 2019). Common implicit modelling methods include nearest neighbour value interpolation (Olivier R. et al.,
2012), inverse distance weighted (IDW) interpolation (Liu H. et al., 2020; Liu Z et al., 2021), discrete smooth interpolation
(DSI) (Mallet J. 1997), kriging (Wang G.W. et al., 2011; Thanh H. V. et al., 2019), the MLS method (Manchuk J. G. et al.,
2019), and the radial basis function (RBF) method (Caumon G. et al., 2013; Hillier M. et al., 2014; Cuomo S. et al., 2017;
Martin R. et al., 2017; Skala et al., 2017; Zhong D. Y. et al., 2019). However, At present, underground 3D data acquisition
methods include borehole exploration technology and applied geophysical technology. Although the cost of borehole
exploration is higher than that of geophysics, its exploration precision is high, making it the main means of high-precision
80 exploration in local areas. Borehole data can intuitively and reliably obtain geological spatial information. 3D geological

modelling from borehole data can be divided into explicit modelling and implicit modelling (Wang et al., 2018). Explicit modelling methods more easily add geological semantic constraints during modelling, the boundary control is more accurate, and the modelling results are more in line with the actual geological laws. However, it is difficult to automatically model complex geological structures such as faults, folds and unconformities, and the modelling is not smooth. Examples include automatic modelling methods based on generalized tri-prism volume elements (Wu, L. X., 2004), section connection methods (Yang et al., 2011), etc. Implicit modelling (Caumon et al., 2012; Hillier et al., 2014) solves the implicit equations of the space surface by selecting the appropriate basis functions and using known points in the space to obtain the implicit surface functions and then uses a 3D surface construction algorithm to express them explicitly. Because there is a certain relationship between the implicit surface shape and the selected basis function form, an implicit modelling method has a certain degree of subjectivity for the final model expression. In addition, implicit modelling requires a high data volume, which requires a large amount of borehole data to establish an accurate model, and solving large-scale equations also requires high hardware requirements. Examples include the kriging method (Che et al., 2019), inverse distance weighting method (Liu et al., 2020), Hermite radial basis function method (Guo et al., 2021), etc. Stochastic simulation methods include transition probability-based (Carle and Fogg, 1997), object-based (Lantuejoul, 2002), process-based (Lancaster and Bras, 2002), truncated Gaussian (Matheron et al., 1987), multivariate Gaussian (Armstrong et al., 2011), implicit boundaries (Ferrer et al., 2021), and multipoint statistics (Mariethoz and Caers, 2014) simulations. At present, multipoint geostatistics (MPS) (Guo et al., 2022) has been developed as a method for boreholes. By establishing a grid and defining a random simulation path according to the simulation grid, the stratum attribute values are determined for the grid according to the borehole distribution of a random simulation path.

the sparsity of borehole data, the complexity of geological bodies or geological phenomena, and the limitations of human cognition and expression lead to uncertainty in the relationship between the geometric form of a 3D geological model and the corresponding geological system (Caumon et al., 2007; Caers, 2011; Pakyuz-Charrier et al., 2018). The construction of 3D geological models by establishing implicit equations cannot effectively address this uncertain relationship.

Machine learning methods have been widely used in 3D geological modelling. Traditional machine learning methods include 3D geological modelling based on support vector machines (SVMs) (Smirnoff et al., 2008; Wang et al., 2014), using the kriging model based potential field method to implicitly model geological structures (Calcagno et al., 2008; Goncalves et al., 2017), using Bayesian methods to estimate the uncertainty of geological models, etc. (de la Varga et al., 2016; Wang, H., 2020). These methods are applied to nonimage data.

Machine learning methods have been widely used in 3D geological modelling, and they are generally applied in unsupervised or supervised 3D geological modelling (Wang et al., 2023). Unsupervised machine learning algorithms (e.g., k-means clustering, self-organizing maps, and Gaussian mixture models) can be used to translate multisource geophysical datasets into 3D lithological models by measuring similarity between properties in feature space (Hellman et al., 2017; Giraud et al., 2020; Whiteley et al., 2021; Zhang et al., 2022). Supervised machine learning algorithms (e.g., random forests and artificial neural networks) can be applied to construct 3D lithological models by training from labelled geophysical and geological datasets (Jia et al., 2021; Lysdahl et al., 2022). Despite obtaining encouraging results with supervised machine learning algorithms, most studies have not addressed the following critical challenges regarding supervised machine learning algorithms for 3D geological modelling:

(1) In the scope of 3D modelling, precise geological information, such as relationship of stratigraphy, and tectonic in study area, revealed by borehole data is much less than not revealed by borehole data. Utilizing the precise information obtained via boreholes as labelled data to predict the correctness of the results in many unknown areas still requires further research.

(2) Labelled geological datasets were mainly composed of borehole data from early exploration phases (Jia et al., 2021; Lysdahl et al., 2022). The number of categories of lithological samples in drilling datasets is commonly imbalanced. A

Formatted: Indent: First line: 0 ch

125 classification dataset with skewed class proportions can influence the performance of machine learning algorithms (Chawla
et al., 2002; Batista et al., 2004). However, there is very little published research that addresses the sample imbalance issue
in the context of training supervised machine learning algorithms for 3D lithological modelling.

130 Compared with machine learning methods, deep learning algorithms improve the ability to learn from mining data and
are often combined with complex geophysical and geochemical data for modelling. Currently, there is a wealth of research
on neural network-based deep learning methods for addressing geological issues such as tectonic recognition (Titos et al.,
2018), mineral identification and classification (Xu and Zhou, 2018), seismic data inversion (Huang et al., 2020), and others.
Furthermore, in the realm of constructing 3D geological models, the deep learning approach using neural networks has also
gradually garnered significant attention from numerous scholars (Laloy et al., 2017; Zhang et al., 2019; Ran et al., 2020;
Zhang et al., 2018; Michael Hillier et al., 2021, 2022; S Avalos and Ortiz, 2020). However, the issue of insufficient training
data has yet to be adequately addressed.

135 Compared with traditional machine learning methods, deep learning improves the ability to read mined data and is often
combined with complex geophysical and geochemical data for modelling. For example, neural networks are trained to
predict geological structures from seismic data (Titos et al., 2018); deep neural networks are used to invert complex binary
geological media (Laloy et al., 2017) and generative adversarial networks are used to generate geological models (Zhang et
al., 2019). Deep learning is used to comprehensively utilize geological, gravity, and aeromagnetic data to intelligently
generate regional 3D geological models, which solves the problem of a long 3D modelling cycle and slow effect (Ran et al.,
2020). By designing a targeted U-Net convolutional neural network model, the automatic identification and classification of
underground ore minerals based on a deep learning algorithm has been realized (Xu and Zhou., 2018). By designing a
geological entity recognition model based on a deep belief network, the problem of structured and standardized processing of
geological entity information in text data was solved (Zhang et al., 2018). When performing seismic inversion on different
data sets, deep learning methods have the potential to obtain higher resolution results than traditional machine learning in the
case of big data (Huang et al., 2020).

140 Borehole data are common data in geological exploration, and the data are generally sparse. Research has been
conducted in the field of geology using machine learning methods from borehole data, which can be divided into those based
on spatial data from boreholes and other data from boreholes. There are mainly two kinds of modelling ideas based on
borehole spatial data: borehole sequence simulation and borehole spatial point simulation. Borehole sequence simulation is
divided into borehole sequence prediction and the prediction of each stratum thickness (Zhou et al., 2019). Borehole spatial
point simulation simulates the lithology of the spatial points sampled by the borehole. This method is compared with the
borehole sequence simulation method. The borehole sequence simulation method has better continuity in the vertical
direction and is not affected by the sampling accuracy, while the lithology simulation of a borehole has higher accuracy in
predicting the borehole lithology (Zhang et al., 2021). Models based on borehole spatial point simulation have different
advantages and disadvantages due to the different input and sampling methods of the model. The borehole is upsampled
according to a certain interval, and each sampling point is used as input (Guo et al., 2019). Strata are generated by randomly
selecting B-spline curve functions based on boreholes, and the voxels of each stratum are used as input (Wang et al 2021).
The constructed model is more accurate, but the model mainly relies on randomly selected B-spline curves. If the
coordinates and starting depth of each stratum drilled are used as input (Kim et al., 2022), although the model accuracy is
lower than that of upsampling, it is not easy to overthrow the order of strata. Studies based on other borehole data include
lithology classification based on borehole core description data (Bressan et al., 2020) and 3D geological modelling based on
described boreholes (Fuentes et al., 2020). In conclusion, among borehole data modelling methods, the lithology prediction
method for spatial points is better, but there are still some problems, such as needing 3D geological models established by
other methods as references, low modelling accuracy, and difficulty in modelling complex geological phenomena.

In this paper, we propose a semisupervised deep learning using pseudolabels (SDLP) algorithm for constructing 3D geological models and to overcome the lack of accurate labelled data. Upsampling is used to resolve label imbalance issues in the training dataset. The shallow borehole data from Shenyang, Liaoning Province, are used to construct 3D geological models using the proposed algorithm. To demonstrate the applicability of SDLP, the accuracy, precision, recall, and F1 score results of SDLP are compared with those of a classic support vector machine (SVM) algorithm based on a test dataset. To further assess the accuracy of SDLP, the profiles of the 3D geological models constructed by SDLP, SVM, and Hermite radial basis function (HRBF) are compared. Furthermore, the SDLP algorithm addresses the uncertainty limitations in the implicit HRBF modelling method.

In this paper, we propose a semisupervised deep learning algorithm using pseudolabels from borehole data for urban engineering 3D geological modelling. Then, the trained model is used to predict the unlabelled grids, and the pseudolabel data with high confidence are added to the unlabelled grids to expand the sample data space. Finally, a final model is obtained by training the labelled data and the pseudolabel data. This method only uses borehole data and can establish a more accurate and complex 3D geological model. We establish a 3D geological model for a complex real geological project, compare it with the implicit HRBF method and SVM method, and analyse the uncertainty of the model.

2. 3D Modelling Method Based on Deep Learning

2.1. Borehole data preprocessing

Table 1. Table of average thickness, maximum thickness, minimum thickness and frequency of occurrence of different strata

	Frequency	Average (m)	Maximum (m)	Minimum (m)
fill	167	1.14	4.1	0.4
Clay-1	128	2.21	6	0.7
Clay-2	58	3.46	9.8	0.5
Clay-3	107	5.94	12.8	0.5
Clay-4	54	2.86	5.8	0.5
Sand-1	25	3.34	8.1	1.2
Stone-1	71	6.30	14	1.3
Stone-2	104	3.91	10	0.5
Stone-3	72	6.22	12.5	1.2
Residual-1	52	10.98	16.1	4.8
Residual-2	50	4.77	13.8	2
Residual-3	44	5.47	13.9	1

A total of 167 boreholes from engineering projects in Shenyang city were used to build the 3D geological model in this study. These boreholes are distributed in a 305×264 m area, with an average spacing of approximately 23 metres between adjacent boreholes. The average depth of the boreholes is 29.5 metres. The minimum thickness of the formations revealed by the boreholes is 0.4 metres, and the maximum thickness is 16.1 metres. The maximum average thickness is 10.98 metres, and the minimum average thickness is 1.14 metres (Table 1). The original borehole data mainly include borehole coordinates (X, Y), elevation, lithological thickness, lithological bottom depth, borehole number, lithological ID, etc.

This paper uses deep learning methods for 3D geological modelling, which can further simplify the modelling problem into a strata classification problem. In this method, the coordinate data and strata depth data obtained from boreholes are used as input vectors, and the lithological attributes of the boreholes are used as output vectors. In this study, the borehole data were simplified into continuous one-dimensional data when creating the dataset. However, there are significant differences in the lengths and frequencies of different formations within the borehole dataset (Table 1). For example, in terms of formation thickness, the maximum thickness is 16.1 m, while the minimum thickness is only 0.4 m. In terms of the formation occurrence frequency, the most frequent label, "fill," occurs 167 times, while the least frequent label, "sand-1," occurs 25

times. This significant difference may lead to the overfitting of the training model and ultimately result in poor training performance. Therefore, preprocessing of the borehole data is needed. An upsampling method is proposed to avoid overfitting in the training model caused by training dataset imbalance in this study.

In deep learning, the problem of classifying borehole data can be further reduced to a problem of classifying strata. We can take the coordinates of a borehole and the borehole depth as the input vector and the stratum attribute of the borehole as the output vector. For 3D geological modelling, the model at the borehole should be as consistent as possible with the stratum information revealed by the current borehole. The original borehole data include the borehole coordinates X , Y , borehole elevation, stratum thickness, stratum bottom depth, borehole label, borehole-stratum label, etc. To increase the amount of data, the borehole data are upsampled. Since the thicknesses of the strata may differ greatly from each other, the data balance will be affected if an equal interval sampling method is used, and the data amount of a thick strata will be much greater than that of a thin strata. As a result, the thick strata will dominate the training network, resulting in the classification of unknown regions. The unknown area will be easier to predict as the stratum thickness attribute. The greater the difference in stratum thickness is, the more misclassification will occur.

Based on the above discussion, an unequal interval sampling method is adopted in this paper (Fig. 1). In the figure, H_{41} - H_{35} represents unequal-interval sampling for each stratum in the borehole, while $H_{41}P_4$ - $H_{35}P_5$ represents unequal-interval sampling for each stratum on the deterministic section. Compared with equal-interval sampling, unequal-interval sampling involves changes to the sampling interval according to the thickness of different strata, thereby ensuring the balance of the sampled data. Otherwise, thinner strata may be difficult to predict or deemed to be outliers due to insufficient sampling. As shown in Figure 1, different colours in the borehole region represent different strata attributes, and the strata data are displayed in strips that are continuously distributed in the vertical direction. The attributes of a single stratum are continuously unique within the corresponding depth interval, and there are no data gaps between strata.

Due to the high reliability of borehole data, they can be directly or indirectly used for the generation of accurate models. By applying the Delaunay principle to borehole position points, a surface triangular irregular network (TIN) is created. This TIN encompasses the fundamental topological relationships between adjacent boreholes. If the stratum attributes of two neighbouring boreholes within each TIN are similar, they are connected to form a deterministic section. To ensure accurate geological predictions and eliminate the influence of distant and loosely correlated borehole connections, narrow triangles are removed from the TIN. This approach, similar to the generalized tri-prism (GTP) model, preserves the internal connectivity among the three corresponding boreholes and enables the simulation of various complex geological phenomena. Once the deterministic sections are connected, unequal interval sampling is conducted both horizontally and vertically, and the sampling density at the borehole locations is balanced to avoid overly dense sampling that may impact network training. The unequal interval sampling formula for borehole data is expressed as Equation (1), and the unequal interval sampling point coordinate formula for deterministic sections is expressed as Equation (2).

Based on the above discussion, an unequal interval sampling method is adopted in this paper. Compared with equal interval sampling, unequal interval sampling changes the sampling interval according to the thickness of each stratum to ensure sampling data balance. At the same time, in the interior of each stratum, equal interval sampling is maintained, and the critical point attributes are preserved. Otherwise, the thinner strata may be difficult to predict or be considered as outliers due to too little sampling. The formula for unequal interval sampling can be expressed as follows:

$$Z_{ij} = \frac{(S_{ij}-S_{ij-1})}{n} \quad (1)$$

$$\begin{cases} P_{ijx} = x_1 + \frac{x_2-x_1}{n}(2j-1) \\ P_{ijy} = y_1 + \frac{y_2-y_1}{n}(2j-1) \\ P_{ijz} = \frac{D_1C_2+A_1C_2P_{ijx}+B_1C_2P_{ijy}-D_2C_1-A_2C_1P_{ijy}-B_2C_1P_{ijy}}{C_1C_2n} \end{cases} \quad (2)$$

Formatted: Subscript

Formatted: Subscript

Formatted: Subscript

Formatted: Subscript

Formatted: Subscript

Formatted: Subscript

where S_{ij} is the bottom depth of the j th stratum in the i th borehole, n is the number of samples from each stratum, and Z_{ij} is the sampling interval of the j th stratum in the i th borehole. P_{ijx} , P_{ijy} , and P_{ijz} represent the x , y , and z coordinates of the sampling point in the i th row and j th column of a section. x_1 , y_1 , x_2 , and y_2 are the coordinates of the two connected boreholes in a section. A_1 , B_1 , C_1 , D_1 , A_2 , B_2 , C_2 , and D_2 are the parameters of the straight-line equations representing the top and bottom boundaries of the strata for the connected boreholes.

where S_{ij} is the bottom depth of the j th stratum in the i th borehole, H_{ij} is the thickness of the j th stratum in the i th borehole, n is the number of samples in each strata, and Z_{ij} is the sampling interval of the j th stratum in the i th borehole.

In the borehole stratigraphic data (Fig. 1), different colours indicate different stratigraphic attributes, and the stratigraphic data are displayed in strips, distributed continuously in the vertical direction, with continuous and unique stratigraphic attributes for depth intervals of individual strata and no data gaps between strata. The unequally spaced sampling on the deterministic section is same as the unequally spaced sampling on the borehole, and unequally spaced sampling is also performed in the horizontal direction.

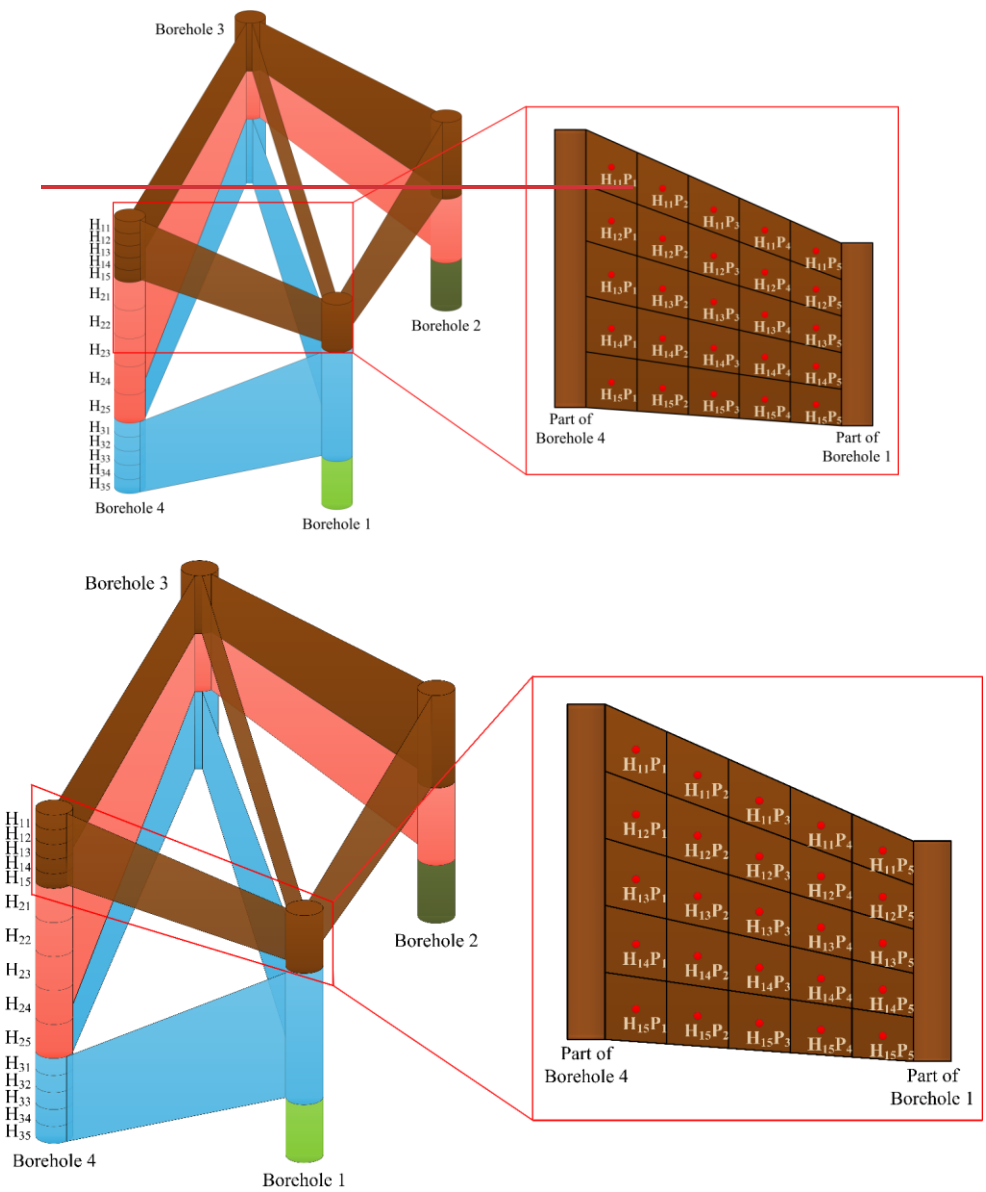


Figure 1. Resampling of borehole data. Upsampling on the boreholes (left); upsampling on the deterministic sections (right).

Borehole data play a direct or indirect role in the generation of the model, and some geological semantic information with high reliability in geology can be obtained through drilling. The borehole data points are inserted point by point according to the Delaunay rule to generate a surface triangular irregular network (TIN), and the basic topological relationship between boreholes is established. Each triangulation consists of three boreholes, and pairs of boreholes with the same attributes are

Formatted: Indent: First line: 0 ch

connected to form a deterministic section. At the same time, long and narrow triangles in the TIN are removed to avoid the connection between the long and narrow triangles that are far away and not related to each other. In this way, the distance between boreholes generated by the Delaunay rule is small. This GTP-like section connection method can maintain the internal connection between the three boreholes and can simulate a variety of complex geological phenomena. At the same time, the modelling scope of this study is mainly for a quaternary sedimentary surface, the possibility of a large stratum inversion phenomenon is low, and the strata are deposited in chronological order. After connecting the deterministic sections, they are sampled at unequal intervals in the both horizontal and vertical directions so that the sampling density is consistent with the borehole to avoid oversampling affecting the training of the network.

The difference in the number of digits between coordinate data (typically 7-8 digits with 3 decimal places) and stratum depth (typically 1-2 digits with 1 decimal place) in borehole data can lead to numerical computation issues in computer systems, making it difficult to train the model and adjust parameters, ultimately affecting the training results of the model. After performing data normalization based on raw data, each indicator is scaled to a specific range, allowing for comprehensive comparative evaluation. To eliminate the influence of digit disparity among input features, ensure the equal impact of different features on model training, and achieve convergence, it is necessary to apply min-max normalization to the data and map the resulting values to the range of 0 to 1. For any dataset x , the mapping function is as follows:

In the borehole data, the order of magnitude between the coordinates and the depth of each stratum is large. This will affect the results of model training, and to eliminate the dimensional influence between the indicators, data normalization is needed to solve the comparability between the data indicators. After the original data are standardized, each index is on the same order of magnitude, which is suitable for comprehensive comparative evaluation. To ensure convergence, the data need to be normalized by mapping the resulting values to [0-1]. For any data x , the mapping function is as follows:

$$x' = \frac{x - x_{\min}}{x_{\max} - x_{\min}} \quad (37)$$

where x_{\max} is the maximum value of the sample data and x_{\min} is the minimum value of the sample data. x' is the normalized result, and x is the input of the model data. Through this normalization method, the convergence speed of the network training model will be improved, the training accuracy will also be improved, and the model training becomes easier.

2.2. Construction of deep neural networks

A single-layer perceptron is one of the simplest feedforward neural networks (Huang et al., 2012), which can be used to simulate partial logic functions and solve linearly separable problems. It cannot classify data sets that are not linearly separable. A multilayer perceptron, by adding N hidden layers between the input layer and the output layer, enhances the model's ability to solve a problem. Multilayer perceptrons have strong robustness, memory ability, and nonlinear fitting

ability, can map complex nonlinear relationships, can deal with a large number of data samples, and have simple learning rules that are easy to implement using computers.

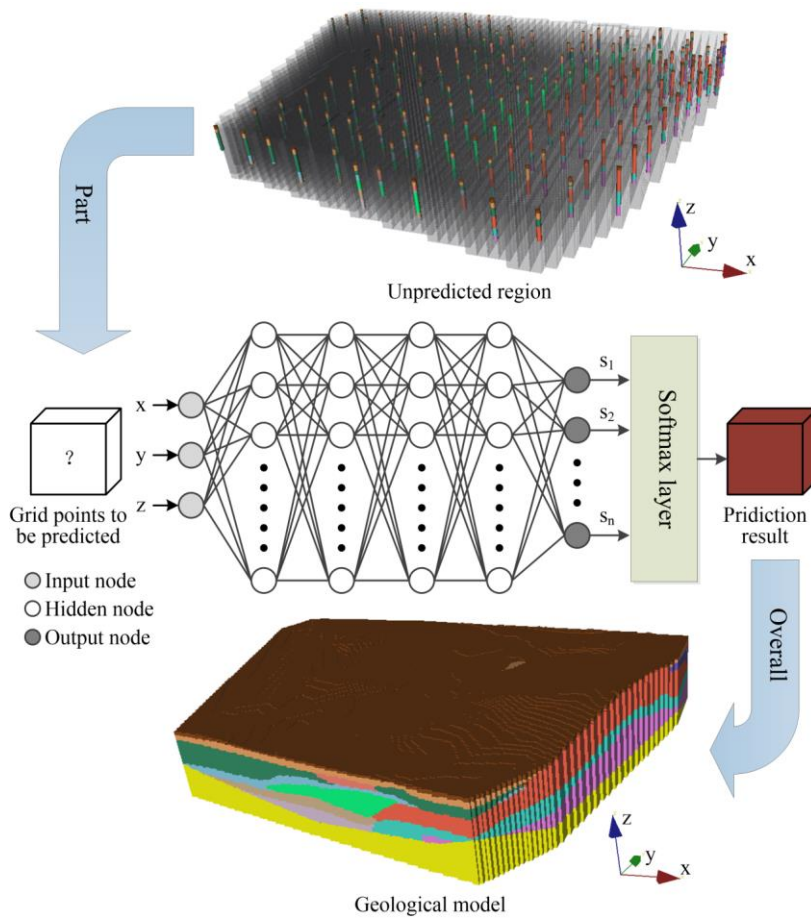
A deep neural network uses the input index and output index to form rules and provides the result closest to the expected output value from the input value, which is a multilayer feedforward neural network according to the error backpropagation algorithm. In a deep neural network, the unit output of the first hidden layer is first calculated, and then the output of the unit in the next layer is used to continue to calculate the output of the unit in the next layer until the output layer outputs the result; this process is called forwards propagation. There is a weight between a deep neural network layer and each layer unit, the initial value of the weight is preset, and the weight of the multilayer perceptron can be trained using the back propagation algorithm. The data in the data set are output after the multilayer perceptron, and the output is compared with the expected value to obtain the corresponding error. The error is backpropagated layer by layer, and the weight of each layer is adjusted accordingly. After a number of adjustments, with the result is a weight that fits the model. The relationship between layers can be expressed as follows: A multilayer perceptron (MLP) is a feedforward artificial neural network that learns to form certain rules through training based on input and output indicators. Thus, results closest to the expected output are obtained after inputting certain values. An MLP is a multilayer feedforward neural network based on the backpropagation algorithm. Each unit between layers in an MLP has a weight with an initial preset value, and unit training is performed using the backpropagation algorithm to adjust the weights between hidden layers. Input data are output after passing data through multiple hidden layers and compared with the expected labels to obtain the corresponding error, which is then propagated layer by layer backwards to adjust the weight of each layer. After multiple adjustments, suitable weights for the model are obtained. The relationship between layers can be expressed as shown in Equation (4). In the network model, the coordinates of each upsampled spatial point in the prediction area, x , y , and z , are used as inputs, and the geological properties of the spatial points are output. Each input represents a spatial feature dimension, and through four fully connected layers, the input data are processed and transformed. Each hidden layer contains multiple nodes, where each node is connected to all nodes in the previous layer. By multiplying by weights and applying an activation function, the input undergoes nonlinear transformation, resulting in expanded dimensionality. This result encompasses the deep features of the sample, and samples of different categories should have different high-dimensional features. The number of neurons in the hidden layer varies according to the complexity of the model, and the rectified linear unit (RELU) activation function is used between hidden layers. To prevent overfitting, a dropout function is added to the penultimate fully connected layers of the network to randomly reduce the number of neurons. Finally, the output value of each category is normalized using the exponential function through a fully connected layer and a softmax layer, and the sum of the probabilities of all categories is 1. The predicted results of each data point are integrated to form the entire 3D geological model (Figure 2). The network

model uses the Adam optimizer, and the loss function adopted is the cross-entropy loss function, which is commonly used in multiclassification tasks.

$$Y_j = \sum_{i=1}^n W_{ij} X_i + b \quad (43)$$

where Y_j is the input of the next layer, W_{ij} is the connection weight from cell X_i of the previous layer to cell Y_j of the next layer, and b denotes the offset value.

In the network model (Fig. 2), the coordinate data x, y, z of each upsampled spatial point in the prediction area are taken as the input, and the stratum attribute of the spatial point is the output. Each input represents a dimensional spatial feature, and after four fully-connected layers, the result of the dimension expansion is obtained by multiplying the weight matrix. It is considered that the result represents the deep characteristics of the sample, and samples of different categories should have different high dimensional features. Through a fully-connected layer and softmax layer, the output value of the category is normalized to the probability of each class after an exponential function change, and the sum of each class is 1. Finally, the predicted results of each data point are integrated to form the entire 3D geological model.



330 **Figure 2. Architecture of a deep neural network. Light grey nodes are input features, dark grey nodes are target outputs, and white nodes are internal network nodes.**

2.3 Semisupervised deep learning algorithm using pseudolabels

335 Compared with that of data from images, point cloud data, etc., borehole data displays a clustered characteristic with local concentrations but overall dispersion tend to be dispersed. Due to the large amount of missing point data between boreholes, it is difficult to accurately express the changing features of stratigraphic boundaries and inclination angles. Supervised learning depends on a large quantity of labelled data to enhance model performance. The labelled data used for training 3D geological models are obtained by upsampling limited borehole points and deterministic borehole profiles. Labelled data associated with spatial grid points in urban areas, which require high modelling precision, are scarce and contain very few features. Therefore, borehole data can be approximately regarded as a large number of missing point data between points, which makes it difficult to accurately express the variation characteristics, such as the inclination angle of the entire stratum interface. Deep learning requires a large amount of labelled data to improve model performance. Only by upsampling the borehole point data and deterministic borehole section data, for the spatial raster points with high modelling accuracy, the data amount is very small and contains very limited features. To effectively solve the labelling problem, semisupervised learning is combined and with deep learning are combined, and a model is constructed using a small amount of labelled data and a large amount of unlabelled data with pseudolabels for prediction. A small amount of labelled data and a large amount of unlabelled grids are used to build a model, which is conducive to expanding the sample space and making up for the lack of geological semantic information provided by single borehole data. This is beneficial for expanding the training data.

340 The attributes of strata are difficult to determine based on a single mathematical formula. Based on the topological relationships established with the TINs of three boreholes, three prisms are constructed using a method similar to the GTP approach by connecting the boreholes based on their stratigraphic properties, and the stratigraphic properties of the interior grid points of the prisms are obtained. For the predicted grid points within the prisms, it is assumed that their stratigraphic properties are similar to the properties of the prism, and when adding pseudolabels, it is assumed that the confidence level for each predicted stratigraphic property is high. Based on this approach, a semisupervised learning method based on pseudolabels is used to generate pseudolabels for the unlabelled data and improve learning performance. First, the model is trained using labelled data. When the model achieves a relatively high accuracy after training for a certain number of rounds, the trained model is used to predict the unlabelled data, and the results predicted with high confidence are selected as the pseudolabels. The pseudolabelled data and labelled data are combined and used in training for a certain number of rounds. The above process is repeated until the proportion of newly added pseudolabelled data in each round is lower than a certain threshold. At this point, high-confidence labels are considered to be obtained, and the model has been sufficiently trained on all data.

360 In the geological field, there is no specific mathematical law for the attribute of strata. The borehole vertex data points from the Delaunay rule of the generated surface are irregular triangle net topological relationships of three boreholes, according to the borehole stratum attribute, they are connected into triangular prisms, then it is considered that the data points in this range have the highest confidence in the stratum attributes determined by the triangular prisms. On this basis, a

semisupervised method using pseudolabels is used to enhance learning by generating pseudolabels for unlabelled grids. First, the model is trained using the labelled data, and when the model reaches a high accuracy after a certain number of training rounds, the trained model is used to predict the unlabelled grids, and the prediction result with higher confidence is selected as the pseudolabel. The pseudolabel data and label data are combined for training. After a certain round of training, the above process is repeated until the new pseudolabel data in each round are less than a certain proportion. At this point, it is considered that most of the grids with high confidence have been labelled, and the model has been trained on the data after data augmentation.

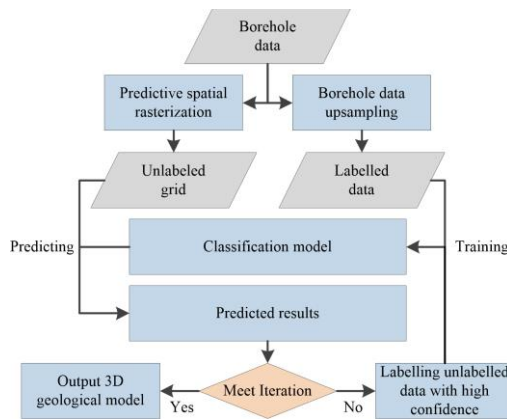


Figure 3. Algorithm flow chart.

2.4. Analysis of model uncertainty

The last layer of the neural network classifier normalizes the probability of the output through the softmax layer, and the softmax normalized result can be approximated as the probability corresponding to each stratum at that a given data point. Therefore, when analysing the uncertainty of each data point of-in the raster model, the normalized information entropy can be introduced to quantitatively evaluate the uncertainty of the geological model. The normalized information entropy formula is as follows:

$$H(X) = - \frac{\sum_{x \in S} p(x) \ln(p(x))}{S_{\max}} \quad (54)$$

where S is the number of possible geological attributes for each data point, S_{max} is equal to ln(n), and n is the number of possible geological attributes. The information entropy of each data point is obtained by calculating the probability p(x) of each data point over all geological attributes. The magnitude of information entropy reflects the degree of complexity at a certain location in the geological model. The closer the information entropy is to 0, the higher the certainty of a data point for a certain stratum attribute, and the closer the information entropy is to 1, the higher the uncertainty of a data point for multiple geological attributes.

In addition, the data can be analysed based on an estimated confusion index (Burrough et al., 1997), and the ambiguity of classification can be evaluated by selecting the results of the two prediction categories with the highest probability for each data point. The confusion index formula is as follows:

$$CI = [1 - (\mu_{\max} - \mu_{\max-1})] \quad (65)$$

where μ_{\max} is the probability of the class with the highest predicted probability and $\mu_{\max-1}$ is the probability of the class with the second highest predicted probability. CI values range from 0-1 to indicate the degree of confusion predicted by thefor a certain data point, with 0 indicating that the_a classification result with a low confusion index is not ambiguous and 1 indicating that the_a classification result with a high confusion index is highly ambiguous.

3. Experimental method and verification

~~To further illustrate the applicability of the proposed method, this chapter uses a practical geological case to conduct 3D geological modelling and analysis with the proposed method. To verify the rationality of the model, the neural network model is compared with a mature implicit modelling method (HRBF). To illustrate the improvement of the modelling effect of the proposed method compared with the traditional 3D modelling method based on machine learning and the relative reliability of the modelling method in geological semantics, the same section of the 3D geological model established using the proposed method and the SVM method is compared. The proposed algorithm is implemented based on the PyTorch open source machine learning library. The SVM algorithm uses the RBF convolution kernel, the parameters are determined by grid search, and the SVM method in the ThunderSvm library is used for training (Wen et al., 2018). The model established using the algorithm mentioned in the experiment is visualized with the developed visualization platform. All test experiments in this chapter are performed on the same device with the following parameters: Intel(R) Core(TM) i7-10750H CPU @2.60 GHz, NVIDIA GeForce RTX 2060, 16.0 GB RAM, Windows 10 (64-bit).~~

~~The Shenyang city 3D geological models were built using the SDLP, SVM, and HRBF algorithms. All test experiments in this chapter were performed on the same device: an Intel(R) Core (TM) i7-10750H CPU @2.60 GHz with an NVIDIA GeForce RTX 2060, 16.0 GB RAM, and Windows 10 (64-bit).~~

~~The ReLU function was used as the activation function in the SDLP algorithm, the initial learning rate was set to 0.001, and the batch size for training was set to 512. When the model training accuracy reached 90% or after 500 epochs, the unlabelled grids were labelled with pseudolabels. When the newly added pseudolabels accounted for less than 10% of the number of grids lacking labels in a given epoch, the model was trained for a total of 2000 epochs more before stopping. The training accuracy and loss values are shown in Fig. 4. The accuracy, precision, recall, and F1 score of the SVM, SDLP, and DL (the neural networks is same with SDLP but without pseudolabel) algorithms for the test dataset are shown in Table 2.~~

Formatted: Indent: First line: 2 ch

In the training process, when the labelled data and pseudolabel data are fused, the boundaries of stratigraphic categories are finely delineated, the final model training accuracy is above 95%, the loss function is close to zero, and the precision of the model for the test set is 98.16%. A confusion matrix is obtained from the test set (Fig. 5), which reflects the reliability of the evaluation results of the model. The classification accuracy of the model is high for all layers. Some strata are more likely to be confused due to being thin, displaying similar boundaries as other strata, or the influence of geological phenomena, such as depositional termination. The receiver operating characteristic curve (ROC) is another performance indicator that summarizes the performance of the binary classification model in the positive class and thus can be used to evaluate the diagnostic ability of the classifier according to the threshold change (Fawcett, 2006). The area under the ROC curve (AUC) (Fig. 6) represents a comprehensive measure of all possible classification thresholds. AUC values greater than 90%, from 75-90%, from 50-75% and less than 50% are considered to represent excellent, good, poor and unacceptable performance, respectively (Ray et al., 2010). The AUC values of the model are all above 90%, indicating that the classification performance of the model is excellent.

Table 2. The accuracy, precision, recall, and F1 score values for SVM and SDLP algorithms based on the test dataset

	Accuracy	Precision	Recall	F1 score
SAM	0.955	0.948	0.940	0.944
SDLP	0.982	0.983	0.980	0.982
DL	0.973	0.967	0.968	0.968

3.1. Overview of the study area

The study area is located in a region of Shenyang District, Liaoning Province, China, which is located in the middle of the Liaohu Plain, Liaoning Province. The region is mainly plains, mountains, and hills concentrated in the northeast, and the terrain slopes gradually from northeast to southwest. There are four large rivers running through it. This region has a temperate monsoon continental climate and four distinct seasons. The average annual temperature is 8°C, the average precipitation is 628 mm, increasing from north to south, and the precipitation is concentrated in summer.

3.2. Modelling results and accuracy verification

The area includes data from 167 boreholes distributed over an area of 305 m×264 m, with adjacent boreholes spaced approximately 23 m apart, an average depth of 29.5 m and a minimum thickness of 0.4 m revealed by the boreholes. The ReLU function is used as the activation function in the neural network, the initial learning rate is set to 0.001, and the batch size for training is set to 512. When the model training accuracy reaches 90% and 500 epochs, the unlabelled grids are labelled with a pseudolabel every 100 epochs. When the newly added pseudolabel data are less than 10% of the unlabelled grids evaluated in an epoch, the model continues to train for a total of 2000 epochs before stopping.

The training accuracy and losses in the method process are shown in Fig. 4. In the training process, when the labelled data and pseudolabel data are fused, the boundary demarcation of stratigraphic categories is more finely delineated, the final model training accuracy is above 95%, the loss function is poor, and the precision of the model on the test set is 98.16%. A confusion matrix is obtained from the test set (Fig. 5), which reflects the evaluation result reliability of the model. The classification accuracy of the model is high for all layers. Some strata are more likely to be confused due to thin strata, similar boundaries with other strata, or more geological phenomena, such as depositional termination. The receiver operating characteristic curve (ROC) is another performance indicator that summarizes the performance of the binary classification model in the positive class and thus evaluates the diagnostic ability of the classifier according to the threshold change (Fawcett, 2006). The area under the ROC curve (AUC) (Fig. 6) represents a comprehensive measure of all possible classification thresholds. AUC values greater than 90%, 75-90%, 50-75% and less than 50% are considered to represent excellent, good, poor and unacceptable performance, respectively (Ray et al., 2010). The AUC values of the model are all above 90%, indicating that the classification performance of the model is excellent.

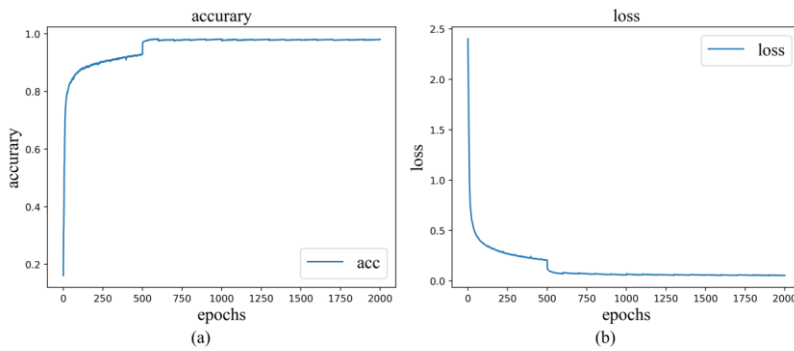
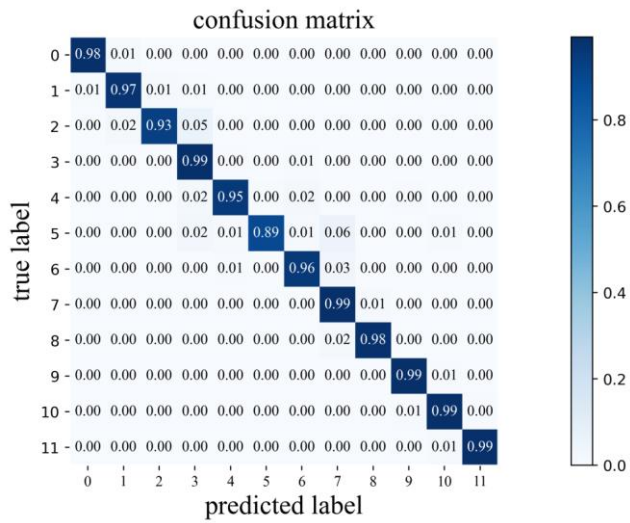
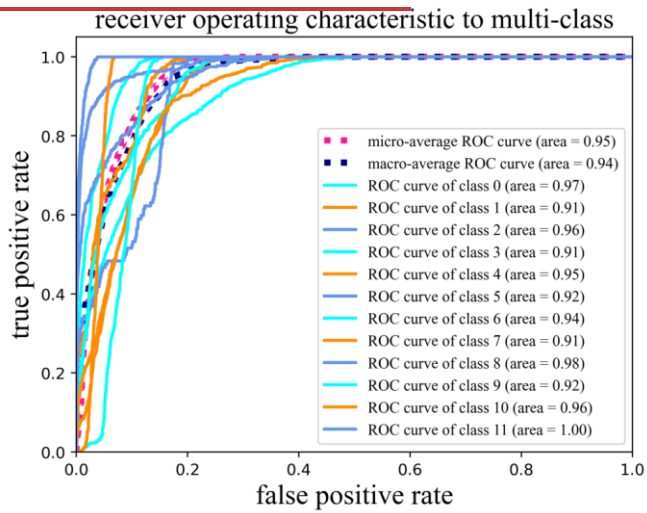


Figure 4. Model training accuracy and loss variation curves.



455

Figure 5. Confusion matrix of the classification results when the model is applied to the test data set.



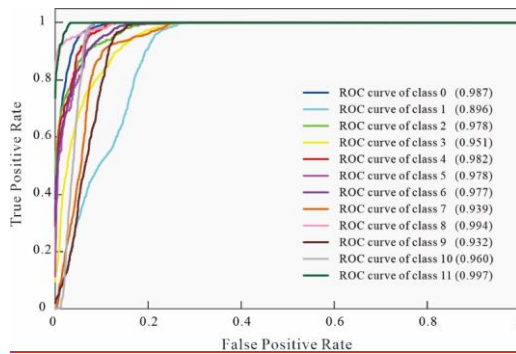


Figure 6. ROC curve for classification.

460 The grid accuracy used in modelling is 1.5 m×1.3 m×0.3 m. The model uses the Tin mesh constructed from the top of boreholes to restrict the surface. The modelling range is determined according to the convex hull established-built by the borehole datas, and the base of the model is determined according to the convex hull established-built by the bottoms of borehole datas. Fig. 7 shows the modelling results of-for the study area. The model reveals the coverage relationships between-among the strata and reproduces the contact relationship between the depositional-termination and unconformity of the strata.

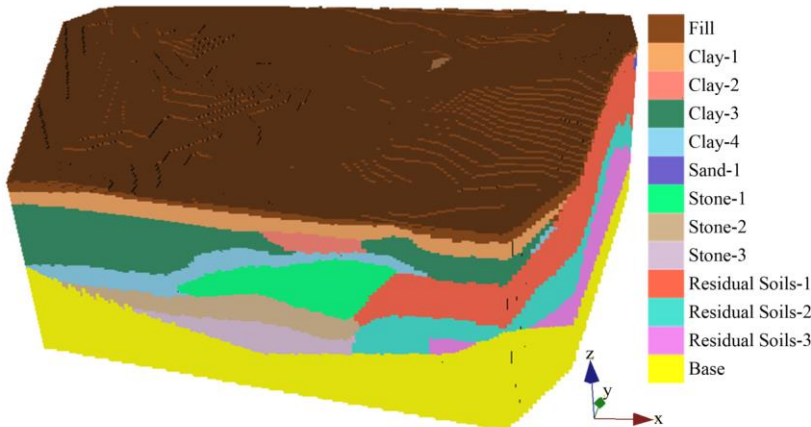


Figure 7. Model built using deep neural networks and the model legend.

470 To test the estimation accuracy of-at nonborehole positions-locations using the proposed method, the borehole data are were divided into a training set and a test set through k-fold cross validation, learning was performed with the training set of borehole data-is learned, and the test set accuracy is-was compared and analysed, where K is-was set to 10.

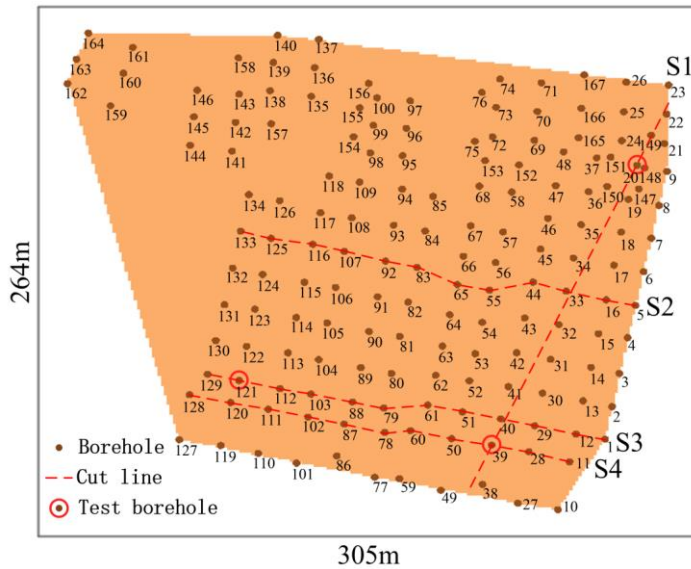


Figure 8. Borehole distribution and experimental analysis of the section line path based on different profiles. The red dotted line is the profile the section route, and the red circled borehole points circled in red correspond to the boreholes tested using K1 in the section.

475 The boreholes in the test set were sampled at equal intervals to determine the data point attributes at the boreholes, and the average accuracy of the k-fold cross validation was calculated to be 71.65%. As there is a certain distance between the boreholes, eliminating an entire borehole will lead to a change in the geological semantic information of the area. When the geological semantic information contained in a borehole is high (Fig. 9), it will be difficult to predict the borehole through the surrounding boreholes, so it is inevitable to obtain poor prediction results when predicting the borehole. Therefore, among the boreholes in the k-fold cross validation, the boreholes that have no more than three depositional terminations between any stratum and the surrounding boreholes and are not at the unconformity boundary are selected for statistical analysis. Among them, the topological relationship of the surrounding boreholes is established using the surface irregular triangulation generated by the Delaunay rule, and the average accuracy is 85.9%. Due to the varying amount of geological information contained in individual borehole data, the importance of different boreholes in constructing the 3D geological model also differs. For instance, the test borehole data contains valuable lens body stratigraphic information and stratigraphic extinction information (Fig. 9). Removing the test borehole data would significantly decrease the accuracy of the prediction results. Therefore, we utilize the surface irregular triangulation method generated by the Delaunay rule to determine the topological relationships between the boreholes. Based on this approach, we ensure that boreholes containing a significant amount of geological information are not excluded during K-fold validation. These operations have improved the accuracy of K-fold validation from 71.65 to 85.9.

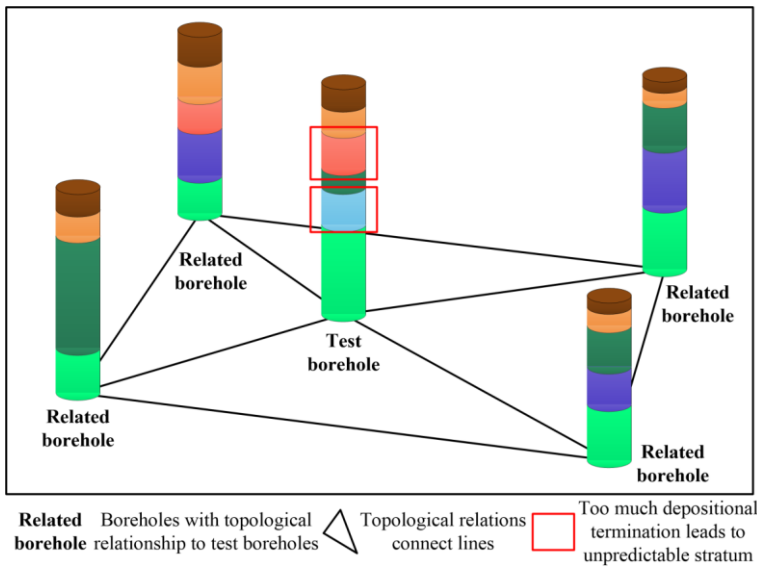


Figure 9. A situation in which too much depositional termination affects the prediction. A related borehole is a borehole that has a topological relationship with the predicted borehole. The red solid-line frame is the stratum, which is difficult to predict due to the excessive occurrence of depositional termination.

495 To further analyse the influence of accuracy on the model, the a model with complete borehole data and the a model
 with excluded sample K1 test borehole data were established, and the sections of the models through a test borehole were
 compared (Fig. 10). The Figure 10 show the The results of straight cutting and cutting along the boreholes are shown for a
 straight line thought the S1 and S3 profiles. Most areas of the sections at the boreholes of in the test set are consistent with
 the sections established built by using a complete borehole. Since some test set boreholes are near the depositional
 500 terminations, there is a certain difference between the model and the data from test boreholes, but the results are still close to
 the original model and reasonable. In summary, it can be considered that the modelling-SDLP method display a good
 prediction ability for has a strong prediction ability for the neighbouring part of boreholes and can reveal the distribution
 characteristics of the stratastratum.

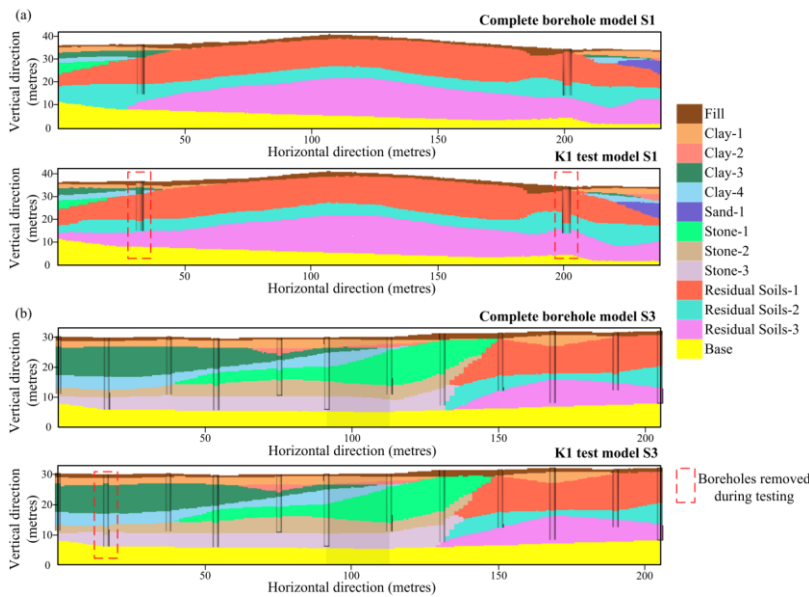


Figure 10. Comparison of the modelling results of sample K1 with the complete drilling results. The dotted box shows the boreholes eliminated considered during the test.

3.3. Comparative analysis of models

To further verify the rationality of the model, the neural network model is compared with a mature implicit modelling method. The modelling method compared in this study is the implicit Hermite radial-basis function (HRBF) 3D geological modelling method. This method uses the implicit Hermite radial-basis function to simulate the stratum interface. Since the implicit model is a vector model, the vector model is transformed into a grid model with the same size as the minimum grid cell of the neural network model for comparison. The implicit model has a thicker base than the deep learning model.

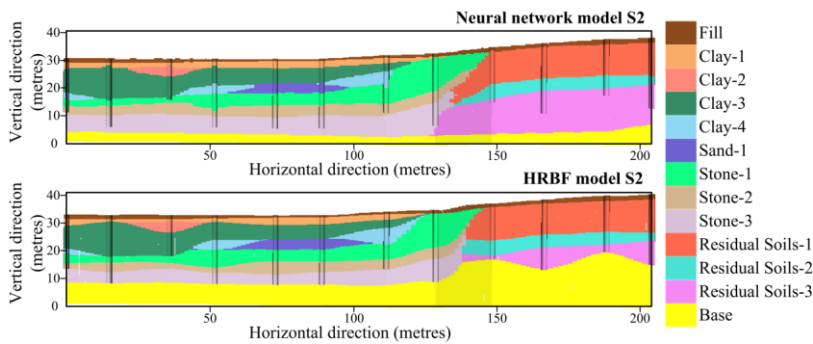


Figure 11. Comparison of the model section between the deep neural network method and the HRBF implicit method.

The deep-learning model and the implicit model are visually consistent along the borehole section (Fig. 11) in terms of the thickness and extension angle of the strata. The implicit model constrains the stratum interface through the control points of each borehole and the implicit equation. The deep-learning model calculates the labelled and pseudolabelled data loss, trains the neural network through backpropagation to obtain the stratigraphic interface, and predicts the stratum data points in the modelling area. Therefore, when there is a depositional termination or unconformity phenomenon, the deep-learning model and the implicit model have certain differences in the depositional termination angle and the thickness change of the stratum. At this time, the shape of the implicit model is mainly determined by the control points determined by the boreholes. However, the machine-learning model predicts using upsampled borehole and pseudolabel data with high confidence, which has certain uncertainty.

To illustrate the improvement of the modelling effect of the proposed method compared with the traditional machine learning 3D modelling method and the relative reliability of the modelling method in geological semantics, previous articles have proven (Guo et al., 2019) that the SVM algorithm has the best modelling effect among traditional machine learning 3D geological modelling methods. Therefore, the section of the 3D geological model established using the proposed method and the SVM method is compared along the borehole section. The proposed algorithm is implemented based on the PyTorch open source machine learning library. The SVM algorithm uses the RBF convolution kernel, the parameters are determined by grid search, and the SVM method in the ThunderSvm library is used for training.

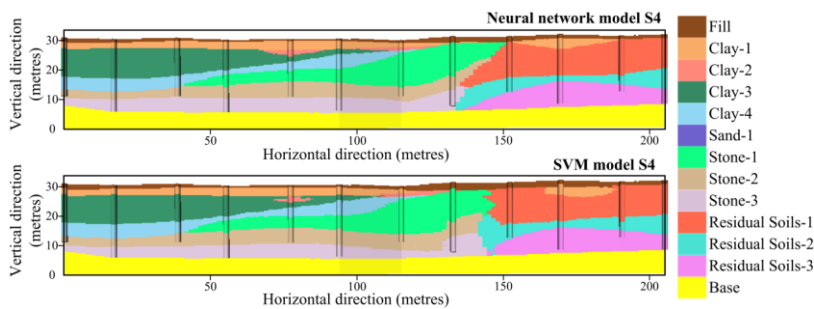


Figure 12. Comparison of the model section between the deep neural network method and the SVM method.

In the study area, the modelling results of the proposed method for complex geological conditions are significantly improved compared with those of the SVM method. By observing the consistency of the attributes of the boreholes and sedimentary strata in Fig. 12, it can be seen that the consistency of the proposed method is higher. In addition, when there is a phenomenon such as depositional termination or unconformity, the variation in thickness and dip angle at the depositional termination or unconformity of the strata modelled using the proposed method is more consistent with the geological semantics. However, the SVM modelling quality decreases significantly when depositional termination or unconformity occurs, and there are many prediction errors or stratum mutation problems. From the model section

comparison, it can be concluded that the proposed method has significantly improved model morphology compared with the traditional machine learning method.

3.4. Analysis of model uncertainty

For each data point in the established model, the information entropy is calculated from the normalized probability distribution. Through 3D visualization of the information entropy model with close raster accuracy, the uncertainty of the constructed model can be quantitatively analysed, and the uncertainty of each position in the model can be clearly reflected.

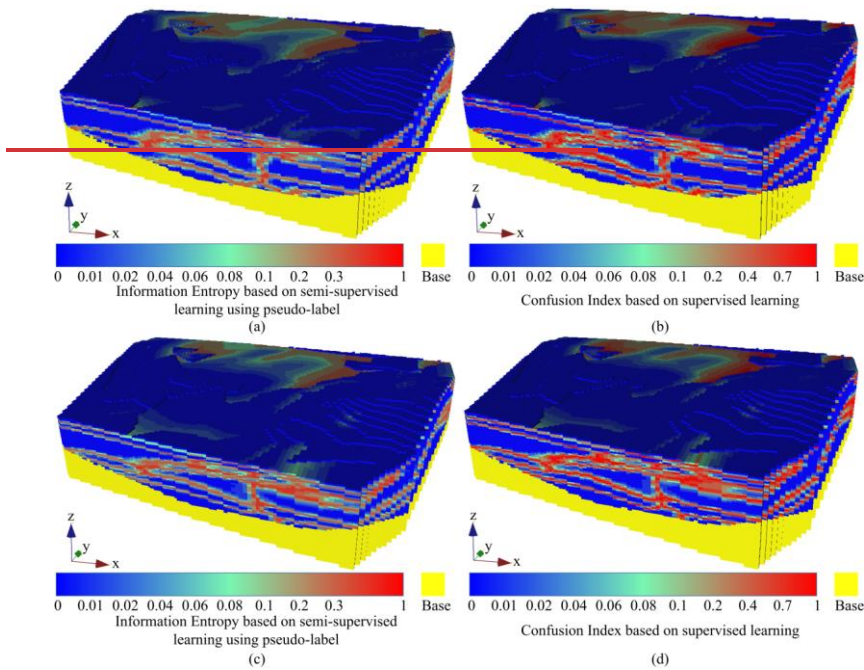


Figure 13. Models of uncertainty: (a) information entropy model based on semisupervised learning using pseudolabels; (b) confusion index model based on semisupervised learning using pseudolabels; (c) information entropy model based on supervised learning; and (d) confusion index model based on supervised learning.

The model (Fig. 13) reflects the uncertainty of the semisupervised learning method using pseudolabels and the supervised learning method to build the model. The blue part of the information entropy model (Fig. 13a, c), where the information entropy is close to 0, means that the uncertainty of the stratum attribute values in the region is low, and the entropy value is small, mainly between the model stratum boundaries. The red part, where the information entropy is close to 1, indicates that the region has a large probability for other stratum attribute values, and the entropy value is large, mainly distributed near the stratum boundary obtained through training. In the confusion index model (Fig. 13b, d), the blue part indicates a low confusion index, and the red part indicates a high confusion index. The overall confusion index of the model

is mostly low, and the confusion index increases significantly at the stratum boundary. By comparing the distribution proportions of the two uncertainty models established using the two learning strategies (Fig. 14 and Fig. 15), the model based on the semisupervised learning method using pseudolabels has lower uncertainty than the model based on the supervised learning method, and the semisupervised learning method using pseudolabels can effectively improve the sample space and improve the stability of the model quality.

From the model part, it can be observed that the information entropy and confusion index increase significantly at the boundary of the unconformity or complex depositional termination phenomenon strata, and the stratum boundary has great uncertainty. The uncertainty will increase obviously only when complex geological phenomena such as stratum interface or deposition termination occur, which indicates that the modelling results are stable and the modelling method is reliable.

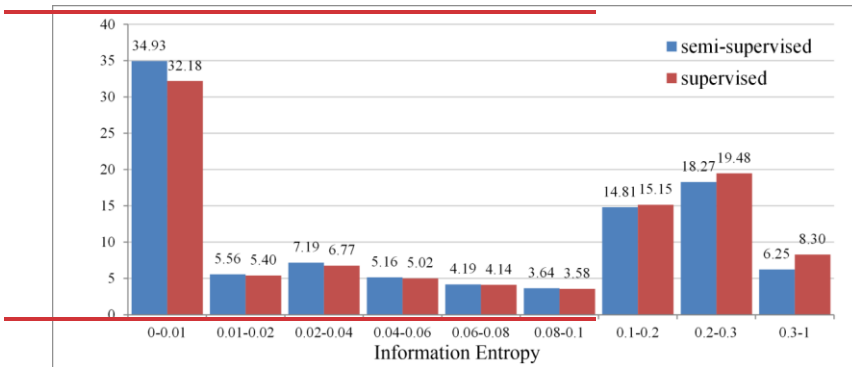


Figure 14. Comparison of the information entropy proportion distribution.

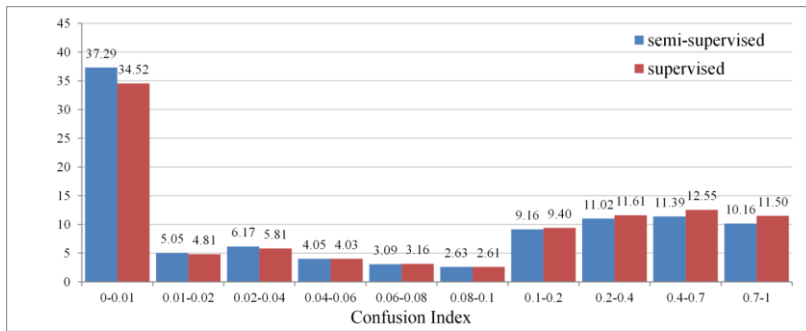


Figure 15. Comparison of the confusion index proportion distribution.

4. Discussion

4.1 Verification of the Accuracy of the HRBF Method

Three-dimensional geological modelling based on the Hermite radial basis function (HRBF) is one kind of implicit function modelling, and implicit modelling methods based on HRBF have been widely used in the modelling of ore bodies, regional geological surveys (Guo et al., 2016), urban geological surveys (Guo et al., 2021), tunnelling projects (Xiong et al., 2018), and volcanic formations (Guo et al., 2020). Therefore, in this paper, the HRBF method is used to build a 3D geological model of Shenyang city, and this model is used to compare the accuracy of the SDLP and SVM algorithms. Before evaluating the accuracy of the two algorithms mentioned earlier, it is essential to conduct an accurate analysis of the 3D geological model constructed using the HRBF method. To demonstrate the accuracy of this approach, we first use the HRBF method to build a 3D geological model of Shenyang city. S1, S2, S3, and S4 are profiles within the 3D geological model of Shenyang city, which contain many geological strata and complex geological relationships. The accuracy of these profiles can effectively reflect the accuracy of the HRBF modelling method. In the S1 geological profile, the stratigraphic boundaries contained in the borehole dataset nearly perfectly correspond to the boundaries of the three-dimensional geological model built based on the HRBF method (Figure. 11). This matching effect is also demonstrated for the S2, S3, and S4 geological profiles. The accurate correspondence between the borehole data and the cross-sections of the 3D geological model indicates the precision of the HRBF modelling method in constructing the three-dimensional geological model. Furthermore, 3D geological models of Shenyang city built using the HRBF method have been verified as effective in engineering applications (Guo et al.,2021). In conclusion, the 3D geological model built using the HRBF method can serve as a standard for evaluating the quality of 3D geological models constructed with the SDLP and SVM algorithms.

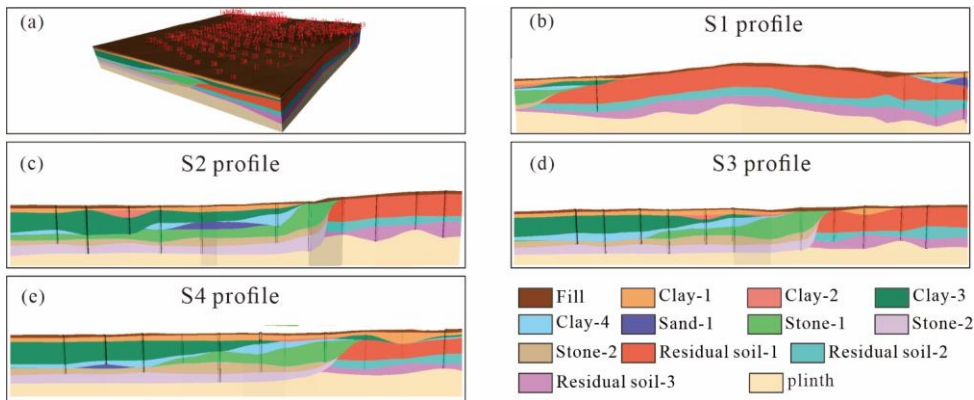


Figure.11 (a) the 3D geological model constructed by HRBF algorithm; (b) the S1 profile built by HRBF algorithm; (c) the S2 profile built by HRBF algorithm; (d) the S3 profile built by HRBF algorithm; (e) the S4 profile built by HRBF algorithm

Formatted: Font: (Default) Times New Roman, (Asian) Times New Roman, 10 pt, Bold, Font color: Auto

Formatted: Font: (Default) Times New Roman, (Asian) Times New Roman, 10 pt, Bold

Formatted: Heading 2, Space Before: 12 pt, After: 12 pt, Line spacing: single

4.2 Comparison of Different Algorithms

Before building the three-dimensional geological model using the SDLP and SVM algorithms, it is necessary to observe the performance of these two algorithms based on the test dataset. According to the prediction results for the test dataset, the accuracy, precision, recall, and F1 score of the SDLP algorithm are 0.982, 0.983, 0.980, and 0.982, respectively, all of which are higher than those of the SVM algorithm (Fig. 12). The reason for these overall results may be that the SDLP algorithm uses more training data, enabling the model to learn patterns with higher generalization ability.

Furthermore, the accuracy, precision, recall, and F1 score of the SDLP algorithm are also higher than those of the DL algorithm (Fig.11). This phenomenon may be attributed to the increased quantity of the training dataset resulting from the use of pseudolabels constructed with the TIN method. The expanded training dataset enables the neural network model to achieve better generalization.

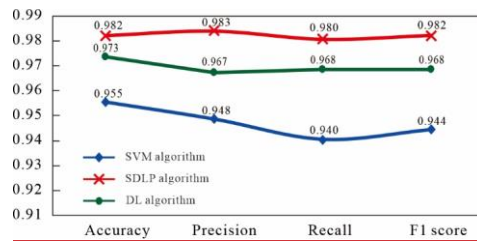


Figure 12. Accuracy, precision, recall, and F1 score of the SDLP and SVM algorithms.

In this paper, we propose a semisupervised learning algorithm using pseudolabels for 3D geological modelling from borehole data. Because the borehole data sampling density is very sparse relative to the modelling range, it is difficult to obtain a stratigraphic interface with high accuracy through supervised learning. However, the modelling area and modelling accuracy of 3D geological modelling are artificial settings, and the distribution of spatial points that need to be predicted and the distribution of boreholes often lack feature connections, so it is difficult to use unsupervised learning from borehole data. In this paper, the accuracy of the stratigraphic interface obtained through training is improved by adding pseudolabel data with high confidence to the unlabelled grids within the modelling scope. This paper also proves that the modelling method is effective and reliable and can reduce the uncertainty through the 3D geological modelling of the Shenyang complex geological area and the uncertainty analysis, and the modelling results are good and basically in accordance with the geological semantics.

Compared with the MPS method, which builds a grid, defines a random simulation path based on the simulation grid, and determines the stratum attribute values for the grid based on the borehole distribution of a random simulation path, the proposed method trains each stratigraphic interface according to the borehole data and the pseudolabel data predicted between the boreholes and determines the attribute value according to the relationship between the predicted area and the stratigraphic interface. It is not difficult to see from the principle of the method that the MPS method pays more attention to

Formatted: Font: (Asian) Times New Roman, Bold, Font color: Auto

Formatted: Font: (Asian) Times New Roman, Bold

Formatted: Heading 2, Space Before: 12 pt, After: 12 pt, Line spacing: single

Formatted: Indent: First line: 2 ch

Formatted: English (United States)

Formatted: Centered

520 the local borehole distribution, while the machine learning method pays more attention to the macroscopic borehole distribution.

The limitation of the method in this paper is that unequal interval sampling is used, which prevents the problem of severe data imbalance leading to missing stratigraphy, but for thicker boreholes, the interval of borehole sampling increases, which leads to a loss of borehole information to some extent, so how to better reconstruct the borehole data is still a problem worth studying.

525 Because the surface irregular triangulation network generated using Delaunay's rule is adopted in this paper to establish the topological relationship between three boreholes, the stratigraphic relationship is used to determine the pseudolabel confidence. When the depth of the borehole bottom fluctuates greatly, it is difficult to determine the pseudolabel confidence under a borehole with very shallow fluctuation, which leads to a decrease in local modelling accuracy.

530 4.3 Comparative Analysis of Models

The profiles of the 3D geological model of Shenyang city are compared to further validate the generalization ability of the SDLP algorithm and the SVM algorithm. The implicit HRBF modelling method exhibits excellent consistency with the borehole data in the profiles, and thus, the profiles constructed with the HRBF method are used as a benchmark for comparison with the profiles generated by machine learning algorithms. In Figure 13, the horizontal axis represents the modelling results of different algorithms for the same geological profile, and the vertical axis represents the geological profiling modelling results of the same algorithm for different geological profiles.

In the S2 geological profile, the 3D geological models built with the HRBF algorithm and the SDLP algorithm demonstrate a high level of consistency with the borehole data. However, the 3D geological model built with the SVM algorithm shows relatively poor correspondence with the borehole data. Furthermore, the morphology of formations in the 3D geological models created with different algorithms is not entirely consistent within the S2 profile. In sedimentary formations without fault structures, the formation boundaries typically undergo gradual changes rather than abrupt changes. The 3D geological models generated using the SDLP algorithm or the HRBF algorithm generally adhere to these geological laws. For instance, the intersection points of the stone-1, stone-2, and stone-3 strata and the residual-1, residual-2, and residual-3 strata in the 3D geological models developed using the SDLP and HRBF algorithms display smooth transitions, aligning well with the sedimentation patterns of sedimentary formations. Conversely, the contact relationships among the strata at these intersections in the 3D geological model built using the SVM algorithm do not conform to the actual sedimentation patterns. Additionally, at the apex of the lens-shaped sand-1 formation, the 3D geological model created with the SVM algorithm is less realistic than the models produced by the HRBF and SDLP algorithms. Guo et al. (2021) demonstrated through 3D geological modelling methods that there are no fault structures in the Shenyang area. This finding implies that the 3D geological model of the S2 profile built with the SVM method is not reasonable. Moreover, the HRBF

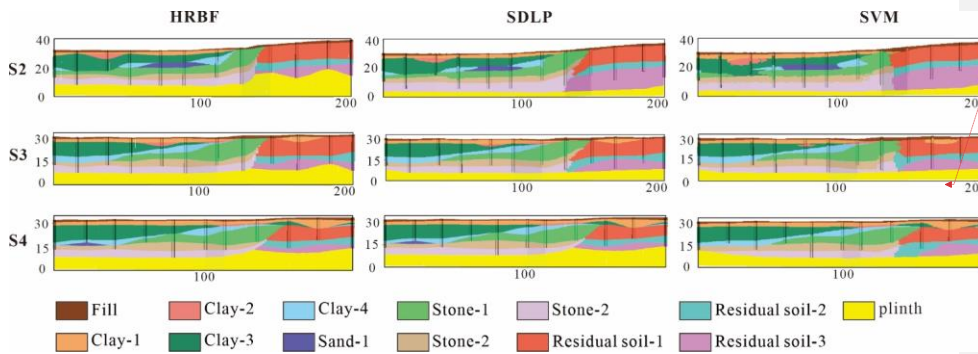
Formatted: Font: (Asian) Times New Roman, Bold, Font color: Auto

Formatted: Font: (Asian) Times New Roman, Bold

Formatted: Heading 2, Indent: First line: 0 ch, Space Before: 12 pt, After: 12 pt, Line spacing: single

Formatted: Indent: First line: 0 ch

method produces modelling results that are deemed unreasonable for the lower two layers, stone-3 and residual-3, due to constraints imposed by the implicit model. These constraints involve the stratum interface being defined based on the control points of each borehole and the implicit equation. In conclusion, for the S2 profile, the SDLP algorithm exhibits the most favourable modelling performance.



Formatted: Left

Figure 13. Geological profiles S2, S3, and S4 for Shenyang city built based on the SDLP, SVM, and HRBF algorithms.

Formatted: Centered

The situation for the S3 and S4 geological profiles is generally similar to that of the S2 profile. The 3D geological models built using the HRBF algorithm and the SDLP algorithm demonstrate a high level of consistency with the borehole data, and the correspondence between the 3D geological model built with the SVM algorithm and the borehole data is comparatively poor. The boundaries of sedimentary formations in the 3D geological models built using the HRBF algorithm or the SDLP algorithm adhere more closely to the actual sedimentation patterns compared to the boundaries of the 3D geological models built using the SVM algorithm. At the lowermost layer boundary, the 3D geological model built using the SDLP algorithm is more reasonable than the one built using the HRBF algorithm.

Based on a comparison of the results of the S2, S3, and S4 profiles, the SDLP algorithm demonstrates better ability to reflect the borehole data when building the 3D geological model. Additionally, the 3D geological model created using the SDLP algorithm better aligns with the sedimentation patterns in terms of the morphology of the formations.

4.4 Analysis of Model Uncertainty

Formatted: Font: (Asian) Times New Roman, Bold, Font color: Auto

For a 3D geological model, only the strata boundary information reflected by borehole data is accurate, and the strata boundaries in areas outside the borehole data region are either artificially inferred or based on constructed basis functions. Therefore, it is necessary to analyse the strata boundaries established based on borehole data in certain areas in the three-dimensional geological model. The implicit HRBF modelling algorithm can be used to effectively visualize borehole data. However, because it is based on implicit basis functions for visualization, it may not effectively process the undisclosed geological information associated with borehole data. In this study, information entropy and a confusion index are introduced to address the HRBF algorithm's inability to consider uncertainty in areas without borehole data. The information

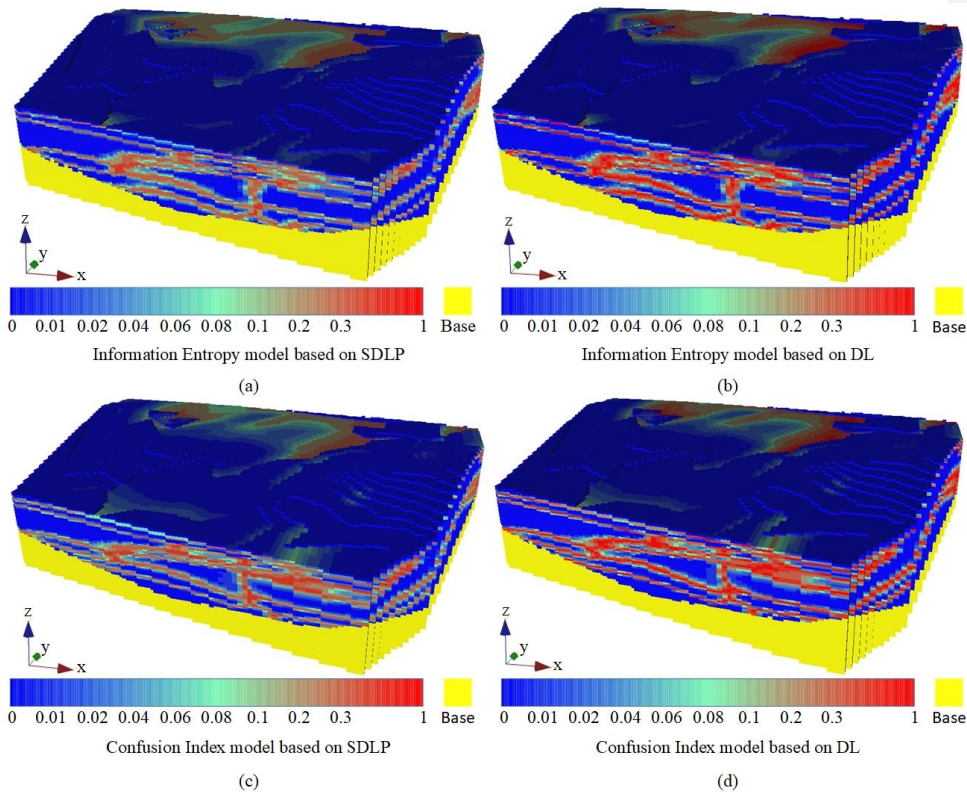
Formatted: Font: (Asian) Times New Roman, Bold

Formatted: Heading 2, Indent: First line: 0 ch, Space Before: 12 pt, After: 12 pt, Line spacing: single

Formatted: Indent: First line: 0 ch

575 entropy is calculated based on the probability distribution of all data points in the normalized model. A visualized
information entropy model can reflect the uncertainty at different locations within the model.

In addition, the results of the information entropy and confusion index models of SDLP and DL algorithms are
580 compared. These results are used to demonstrate the impact of pseudolabelling on the stability of building 3D geological
models using neural network methods.



580 Figure 14. Models of uncertainty: (a) information entropy model based on SDLP; (b) information entropy model based
on DL; (c) confusion index model based on SDLP; and (d) confusion index model based on DL

The information entropy and confusion index models reflect the uncertainty of the semisupervised learning method
585 using pseudolabels and the supervised learning method used to build the models (Fig. 14). The blue part of the information
entropy model (Fig. 14a, c), where the information entropy is close to 0, indicates that the uncertainty of the stratum attribute
values in the region is low, and the entropy value is small, mainly between the model stratum boundaries. The red part,
where the information entropy is close to 1, indicates that the region has a high probability of being influenced by stratum
attribute values, and the entropy value is large, mainly distributed near the stratum boundary obtained through training. In

the confusion index model (Fig. 14b, d), the blue part indicates a low confusion index, and the red part indicates a high confusion index.

In the confusion index model, the three-dimensional geological models built by SDLP algorithm and DL algorithm both exhibit a confusion index close to 0 within strata but increases in the confusion index at the boundaries of the strata. The difference lies in the fact that at the boundaries of strata, the confusion index of the three-dimensional geological model built with the deep learning algorithm without pseudolabelling is closer to 1, indicating lower accuracy than that of the 3D geological model built with the deep learning algorithm with pseudolabelling. Additionally, the information entropy model exhibits similar characteristics to the confusion index model. To visually illustrate the differences between the 3D geological models constructed by the SDLP algorithm and the DL algorithm in terms of information entropy and confusion index, the number of stable grids (with information entropy ranging from 0 to 0.01 and confusion index ranging from 0 to 0.01, Fig.15a, b) and unstable grids (with information entropy ranging from 0.3 to 1 and confusion index ranging from 0.3 to 1, Fig.15a, b) are recorded and compared. The results show that compared to the DL algorithm, the 3D geological model constructed by the SDLP algorithm has a higher proportion of stable grids and a lower proportion of unstable grids. The findings demonstrate that utilizing the TIN algorithm to construct pseudolabels can enhance the stability of the model.

The information entropy and confusion index models can be used to overcome the HRBF algorithm's inability to consider uncertainty, and the results demonstrate that the SDLP algorithm is superior to the deep learning algorithm without pseudolabelling for constructing 3D geological models from the perspectives of information entropy and the confusion index.

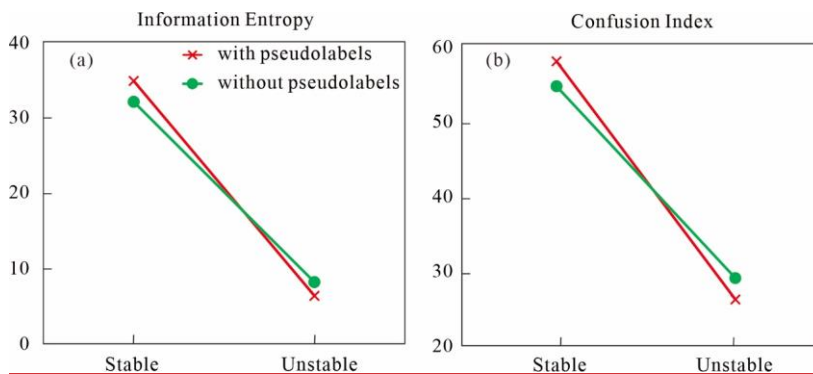


Figure 15. Line plot of information entropy(a) and confusion index (b).

Formatted: Centered

5. Conclusion

In this study, we propose semisupervised deep learning using a pseudolabelling algorithm to build a 3D geological model based on borehole data. By labelling the grid data with high accuracy using the explicit TIN modelling method, we address the lack of labelled training data for building deep learning models. The original data for this study are from engineering

borehole dataset from Shenyang city, and 3D geological models of Shenyang city were constructed using the SDLP, SVM, and HRBF algorithms. The SDLP algorithm achieved an accuracy of 98.16% for the test dataset, outperforming a classic SVM machine learning algorithm. Moreover, the 3D geological model constructed using the SDLP algorithm accurately reflects the boundaries of the formations in the borehole data and aligns well with the real sedimentation patterns. the 3D geological models built with the SDLP algorithm resolve the inability of the implicit HRBF modelling algorithm to consider uncertainty. In conclusion, the proposed SDLP algorithm provides a solution for the lack of training data in deep learning and fills the gap of the HRBF method regarding uncertainty.

In this study, we propose a semisupervised deep learning algorithm using pseudolabels for 3D geological modelling from borehole data. By predicting the pseudolabel for an unlabelled grid within the modelling scope, a 3D geological model is established by expanding the amount of sample data. The proposed method takes the engineering data of Shenyang City as an example to establish a 3D geological model. The accuracy of the deep neural network training model on the test set for sampling data points reaches 98.16%. When the test borehole data without missing geological semantics are predicted through cross validation, the prediction accuracy of the borehole stratum can reach 85.9%. This shows that the established model conforms to the borehole distribution and has good prediction ability. Compared with the implicit HRBF modelling method and SVM modelling method, the modelling results can express the stratum distribution well, and the modelling results are more accurate than those of the traditional machine learning method. The model uncertainty analysis shows that the pseudolabel method can slightly reduce the uncertainty of the model, which can improve the stability of the 3D geological model and has more advantages in dealing with more complex geological phenomena.

Code availability. The ~~program~~ PDNN² was written in the Python programming language. The program reads borehole data and preprocesses the borehole data with upsampling and ~~normalization~~ normalization. By using the DNN to train the model and predict the attributes of data ~~points~~ points, Pseudolabels with high confidence ~~scores were~~ are added to the unlabelled grid points. The code is available for download from the following public repository: <https://zenodo.org/doi/10.5281/zenodo.7833370>.

Data availability. The model data and terrain data ~~of~~ used in the case study in this paper are available at: <https://doi.org/10.5281/zenodo.7535214>.

Video supplement. We have provided web links to download the video recordings of our case studies. The ~~real-area~~ case study of a real area verifies the feasibility of the proposed approach. The video supplement can be viewed at: <https://drive.google.com/file/d/13VERDXM6YJmP7xMabQy3lJhCEXuQSWzk/view?usp=sharing>.

Author contributions. Xuechuang Xu and Jiateng Guo conceived the manuscript; Jiateng Guo provided funding support and ideas; Xuechuang Xu was responsible for the research method and program development; Jiateng Guo provided the data used in this research;

Xuechuang Xu, Jiateng Guo, Xulei Wang, Lixin Wu, Mark Jessell, Zhibin Liu and Yufei Zheng helped to improve the manuscript; [Luyuan Wang helped modified the manuscript](#). All authors have read and agreed to the published version of the manuscript.

Competing interests. The authors declare that they have no known competing financial interests or personal relationships that could appear to have influenced the work reported in this paper.

Acknowledgements. This work was financially supported by the National Natural Science Foundation of China [grant number: 42172327] and the Fundamental Research Funds for the Central Universities [grant number: N2201022].

References

[Avalos, S., & Ortiz, J. M.: Recursive Convolutional Neural Networks in a Multiple-Point Statistics Framework, Computers & Geosciences, 141, 104522, <http://doi.org/https://doi.org/10.1016/j.cageo.2020.104522>, 2020.](#)

[Armstrong, M., Galli, A., Beucher, H., Loc'h, G., Renard, D., Doligez, B., Eschard, R., and Geffroy, F.: Plurigaussian simulations in geosciences, Springer Science & Business Media, 2011.](#)

[Bressan, T.S., de Souza, M.K., Girelli, T.J. and Chemale, F.: Evaluation of machine learning methods for lithology classification using geophysical data, Computers & Geosciences, 139, <https://doi.org/10.1016/j.cageo.2020.104475>, 2020.](#)

[Batista, G. E. A. P., Prati, R. C., & Monard, M. C.: A Study of the Behavior of Several Methods for Balancing Machine Learning Training Data. Sigkdd Explor. Newsl., 6\(1\), 20-29. <http://doi.org/10.1145/1007730.1007735>, 2004](#)

[Burrough, P.A., vanGaans, P.F.M. and Hootsmans, R.: Continuous classification in soil survey: Spatial correlation, confusion and boundaries, GEODERMA, 77\(2-4\): 115-135, \[https://doi.org/10.1016/S0016-7061\\(97\\)00018-9\]\(https://doi.org/10.1016/S0016-7061\(97\)00018-9\), 1997.](#)

[Caers, J. Modeling Uncertainty in the Earth Sciences. Wiley., 2011.](#)

[Calcagno, P., Chiles, J.P., Courrioux, G. and Guillen, A.: Geological modelling from field data and geological knowledge Part I. Modelling method coupling 3D potential-field interpolation and geological rules, Physics of the Earth and Planetary Interiors, 171\(1-4\): 147-157, <https://doi.org/10.1016/j.pepi.2008.06.013>, 2008.](#)

[Caumon, G., L. Tertois, A., & Zhang, L.: Elements for Stochastic Structural Perturbation of Stratigraphic Models, European Association of Geoscientists & Engineers, <http://doi.org/https://doi.org/10.3997/2214-4609.201403041>, 2007.](#)

[Carle, S.F. and Fogg, G.E.: Modeling spatial variability with one and multidimensional continuous-lag Markov chains, MATHEMATICAL GEOLOGY, 29\(7\): 891-918, 1997.](#)

[Caumon, G., Gray, G., Antoine, C. and Titeux, M.O.: Three-Dimensional Implicit Stratigraphic Model Building From Remote Sensing Data on Tetrahedral Meshes: Theory and Appli](#)

770 cation to a Regional Model of La Popa Basin, NE Mexico, IEEE Transactions on Geoscience and Remote Sensing, 51(3):

1613-1621, <https://doi.org/10.1109/TGRS.2012.2207727>, 2013.

775 [Chawla, N. V., Bowyer, K. W., Hall, L. O., & Kegelmeyer, W. P.: Smote: Synthetic Minority Over-Sampling Technique. J. Artif. Int. Res., 16\(1\), 321-357., 2002.](#)

[Che, D. F., Wu, L. X., & Yin, Z. R.: 3D Spatial Modeling for Urban Surface and Subsurface Seamless Integration, 2009 Ieee International Geoscience and Remote Sensing Symposium, Vols 1-5, 1694, <http://doi.org/10.1109/IGARSS.2009.5417787>, 2009.](#)

[Chen, G., Zhu, J., Qiang, M., & Gong, W.: Three-Dimensional Site Characterization with Borehole Data – a Case Study of Suzhou Area, Engineering Geology, 234, 65-82, <http://doi.org/https://doi.org/10.1016/j.enggeo.2017.12.019>, 2018.](#)

[Cuomo, S., Galletti, A., Giunta, G., & Marcellino, L.: Reconstruction of Implicit Curves and Surfaces Via Rbf Interpolation, Applied Numerical Mathematics, 116, 157-171, <http://doi.org/https://doi.org/10.1016/j.apnum.2016.10.016>, 2017.](#)

780 [de la Varga, M., Schaaf, A., & Wellmann, F.: Gempy 1.0: Open-Source Stochastic Geological Modeling and Inversion, Geoscientific Model Development, 12\(1\), 1-32, <http://doi.org/10.5194/gmd-12-1-2019>, 2019.](#)

[Che, D.F. and Jia, Q.R.: Three Dimensional Geological Modeling of Coal Seams Using Weighted Kriging Method and Multi Source Data, IEEE Access, 7: 118037-118045, <https://doi.org/10.1109/ACCESS.2019.2936811>, 2019.](#)

785 [de la Varga, M. and Wellmann, J.F.: Structural geologic modeling as an inference problem: A Bayesian perspective, Interpretation a Journal of Subsurface Characterization, 4\(3\): Sm1-Sm16, 2016.](#)

[Fawcett, T.: An introduction to ROC analysis, Pattern Recognition Letters, 27\(8\): 861-874, 2006.](#)

[Ferrer, R., Emery, X., maleki tehrani, M. and Navarro, F.: Modeling the Uncertainty in the Layout of Geological Units by Implicit Boundary Simulation Accounting for a Preexisting Interpretive Geological Model, Natural Resources Research, 30: 1-23, <https://doi.org/10.1007/s11053-021-09964-9>, 2021.](#)

790 [Fuentes, I., Padarian, J., Iwanaga, T. and Vervoort, R.W.: 3D lithological mapping of borehole descriptions using word embeddings, Computers & Geosciences, 141, <https://doi.org/10.1016/j.cageo.2020.104516>, 2020.](#)

[Gonealves, I.G., Kumaira, S. and Guadagnin, F.: A machine learning approach to the potential field method for implicit modeling of geological structures, Computers & Geosciences, 103: 173-182, <https://doi.org/10.1016/j.cageo.2017.03.015>, 2017.](#)

795 [Guo, J.T., Liu, Y.H., Han, Y.F. and Wang, X.L.: Implicit 3D Geological Modeling Method for Borehole Data Based on Mechine Learning, Journal of Northeastern University \(Natural Science\), 40\(9\): 1337-1342, <https://doi.org/10.12068/j.issn.1005-3026.2019.09.021>, 2019.](#)

- 800 Guo, J.T., Wang, X.L., Wang, J.M., Dai, X.W., Wu, L.X., Li, C.L., Li, F.D., Liu, S.J. and Jessell, M.W.: Three-dimensional geological modeling and spatial analysis from geotechnical borehole data using an implicit surface and marching tetrahedra algorithm, *Engineering Geology*, 284, <https://doi.org/10.1016/j.enggeo.2021.106047>, 2021.
- Guo, J., Wang, Z., Li, C., Li, F., Jessell, M.W., Wu, L. and Wang, J.: Multiple-Point Geostatistics-Based Three-Dimensional Automatic Geological Modeling and Uncertainty Analysis for Borehole Data, *Natural Resources Research*, 31(5): 2347-2367, <https://doi.org/10.1007/s11053-022-10071-6>, 2022.
- 805 Hillier, M.J., Schetselaar, E.M., de Kemp, E.A. and Perron, G.: Three-Dimensional Modelling of Geological Surfaces Using Generalized Interpolation with Radial Basis Functions, *Mathematical Geosciences*, 46(8): 931-953, <https://doi.org/10.1007/s11004-014-9540-3>, 2014.
- ~~Huang, G.B., Zhou, H.M., Ding, X.J. and Zhang, R.: Extreme Learning Machine for Regression and Multiclass Classification, *IEEE Transactions on Systems Man and Cybernetics Part B Cybernetics*, 42(2): 513-529, <https://doi.org/10.1109/TSMCB.2011.2168604>, 2012.~~
- 810 Huang, X.R., Dai, Y., Xu, Y.G. and Tang, J.: Seismic Inversion Experiments Based on Deep Learning Algorithm Using Different Datasets, *Journal of Southwest Petroleum University (Science & Technology Edition)*, 42(6): 16-25, 2020.
- ~~Kim, H. S. and Ji, Y.: Three dimensional geotechnical layer mapping in Seoul using borehole database and deep neural network based model, *Engineering Geology*, 297: 106489, 2022.~~
- 815 Laloy, E., Herault, R., Lee, J., Jacques, D. and Linde, N.: Inversion using a new low-dimensional representation of complex binary geological media based on a deep neural network, *Advances in Water Resources*, 110: 387-405, <https://doi.org/10.1016/j.advwatres.2017.09.029>, 2017.
- Lancaster, S.T. and Bras, R.L.: A simple model of river meandering and its comparison to natural channels, *HYDROLOGICAL PROCESSES*, 16(1): 1-26, <https://doi.org/10.1002/hyp.273>, 2002.
- Lantuéjoul, C.: Geostatistical simulation: models and algorithms (No. 1139), Springer Science & Business Media, 820 <https://doi.org/10.1007/978-3-662-04808-5>, 2001.
- Liu, H., Chen, S.Z., Hou, M.Q. and He, L.: Improved inverse distance weighting method application considering spatial autocorrelation in 3D geological modeling, *Earth Science Informatics*, 13(3): 619-632, <https://doi.org/10.1007/s12145-019-00436-6>, 2020.
- ~~Mariethoz, G. and Caers, J.: Multiple point geostatistics: stochastic modeling with training images, John Wiley & Sons, <https://doi.org/10.1002/9781118662953>, 2014.~~
- ~~Matheron, G., Beucher, H., de Fouquet, C., Galli, A., Guerillot, D. and Ravenne, C.: Conditional Simulation of the Geometry of Fluvio-Deltaic Reservoirs, *Soc. Petrol. Eng. (SPE)*, 16753, <https://doi.org/10.2118/16753-MS>, 1987.~~

- Ran, X.J. and Xue, L.F.: The research of method and system of regional three-dimensional geological modeling, Doctor Thesis, Jilin University, 2020.
- 830 Ray, P., Manach, Y.L., Riou, B. and Houle, T.T.: Statistical evaluation of a biomarker, *Anesthesiology*, 112(4): 1023-1040, <https://doi.org/10.1097/ALN.0b013e3181d47604>, 2010.
- ~~Smirnov, A., Bolsvert, E. and Paradis, S.J.: Support vector machine for 3D modelling from sparse geological information of various origins, *Computers & Geosciences*, 34(2): 127-143, <https://doi.org/10.1016/j.cageo.2006.12.008>, 2008.~~
- 835 Titos, M., Bueno, A., Garcia, L. and Benitez, C.: A Deep Neural Networks Approach to Automatic Recognition Systems for Volcano-Seismic Events, *IEEE Journal of Selected Topics in Applied Earth Observations and Remote Sensing*, 11(5): 1533-1544, <https://doi.org/10.1109/JSTARS.2018.2803198>, 2018.
- ~~Wang, G.C., Carr, T.R., Ju, Y.W. and Li, C.F.: Identifying organic-rich Marcellus Shale lithofacies by support vector machine classifier in the Appalachian basin, *Computers & Geosciences*, 64: 52-60, <https://doi.org/10.1016/j.cageo.2013.12.002>, 2014.~~
- 840 ~~Wang, H.: Finding patterns in subsurface using Bayesian machine learning approach, *Underground Space*, 5(1): 84-92, <https://doi.org/10.2172/1467315>, 2020.~~
- ~~Wang, J.H., Li, N., Zhang, X.R. and Su, X.: 3D soil layer reconstruction of deep foundation pit based on machine learning, *Journal of Chongqing University*, 44(5): 135-145, 2021.~~
- 845 Wang, J.M., Zhao, H., Bi, L. and Wang, L.G.: Implicit 3D Modeling of Ore Body from Geological Boreholes Data Using Hermite Radial Basis Functions, *Minerals*, 8(10), <https://doi.org/10.3390/min8100443>, 2018.
- ~~Wen, Z.Y., Shi, J.S., Li, Q.B., He, B.S. and Chen, J.: ThunderSVM: A Fast SVM Library on GPUs and CPUs, *Journal of Machine Learning Research*, 19, 2018.~~
- Wu, L.X.: Topological relations embodied in a generalized tri-prism (GTP) model for a 3D geoscience modeling system, *Computers & Geosciences*, 30(4): 405-418, <https://doi.org/10.1016/j.cageo.2003.06.005>, 2004.
- 850 Xu, S.T. and Zhou, Y.Z.: Artificial intelligence identification of ore minerals under microscope based on deep learning algorithm, *Acta Petrologica Sinica*, 34(11): 3244-3252, 2018.
- Yang, Y.S., Li, Y.Y., Liu, T.Y., Zhan, Y.L. and Feng, J.: Interactive 3D forward modeling of total field surface and three-component borehole magnetic data for the Daye iron-ore deposit (Central China), *Journal of Applied Geophysics*, 75(2): 254-263, <https://doi.org/10.1016/j.jappgeo.2011.07.010>, 2011.
- 855 Zhang, T.F., Tilke, P., Dupont, E., Zhu, L.C., Liang, L. and Bailey, W.: Generating geologically realistic 3D reservoir facies models using deep learning of sedimentary architecture with generative adversarial networks, *Petroleum Science*, 16(3): 541-549, <https://doi.org/10.1007/s12182-019-0328-4>, 2019.

Zhang, X.Y., Ye, P., Wang, S. and Du, M.: Geological entity recognition method based on Deep Belief Networks, *Acta Petrologica Sinica*, 34(2): 343-351, 2018.

860 Zhang, Y. and Chu, B.Z.: Automatic Borehole Comparison Technology Based on Machine Learning, Master Thesis, China University of Geosciences (Beijing), 2021.

Zhang, Z., Wang, G., Carranza, E. J. M., Yang, S., Zhao, K., Yang, W., & Sha, D.: Three-Dimensional Pseudo-Lithologic Modeling Via Adaptive Feature Weighted K-Means Algorithm From Multi-Source Geophysical Datasets, Qingchengzi Pb-Zn-Ag-Au District, China. *Natural Resources Research*, 31(4), 2163-2179, <http://doi.org/10.1007/s11053-021-09927-0>, 2022.

865 Zhang, Z., Wang, G., Carranza, E. J. M., Liu, C., Li, J., Fu, C., Liu, X., Chen, C., Fan, J., & Dong, Y.: An Integrated Machine Learning Framework with Uncertainty Quantification for Three-Dimensional Lithological Modeling From Multi-Source Geophysical Data and Drilling Data. *Engineering Geology*, 324, 107255. <http://doi.org/10.1016/j.enggeo.2023.107255>, 2023.

870 Zhou, C.Y., Ouyang, J.W., Ming, W.H., Zhang, G.H., Du, Z.C. and Liu, Z.: A Stratigraphic Prediction Method Based on Machine Learning, *Applied Sciences-Basel*, 9(17), 2019.